Geomorphology 240 (2015) 83–101

Contents lists available at ScienceDirect

Geomorphology

journal homepage: www.elsevier.com/locate/geomorph

Paleohydrology of Eberswalde crater, Mars

Rossman P. Irwin III [a,*], Kevin W. Lewis [b], Alan D. Howard [c], John A. Grant [a]

[a] Center for Earth and Planetary Studies, National Air and Space Museum, Smithsonian Institution, MRC 315, 6th St. at Independence Ave. SW, Washington, D.C. 20013, USA
[b] Department of Earth and Planetary Sciences, Johns Hopkins University, Baltimore, MD 21218
[c] Department of Environmental Sciences, University of Virginia, P.O. Box 400123, Charlottesville, VA 22904-4123, USA

ARTICLE INFO

Article history:
Received 23 September 2013
Received in revised form 26 September 2014
Accepted 8 October 2014
Available online 24 October 2014

Keywords:
Mars
Lake
Hydrology
Eberswalde
Holden

ABSTRACT

Eberswalde crater, Mars, contains a well-preserved fluvial distributary network in a likely deltaic setting. The meandering inverted paleochannels and closed drainage basin of this deposit support relatively well constrained estimates of channel-forming discharge (over an individual event flood timescale), runoff production (event and annual timescales), and longevity of deposition (geologic timescale) during the Late Hesperian to Early Amazonian Epochs. The width and meander dimensions of two inverted paleochannels reflect the channel-forming discharge from event floods (~200 to 400 m^3/s), the deposit surface indicates the level (−1400 to −1350 m) and surface area (410 to 810 km^2) of the likely paleolake, and the topography and mapped extent of tributaries constrain the watershed area (5000 to 17,000 km^2). Based on these results and terrestrial empirical constraints on evaporation and sediment concentration, we evaluated three hypothetical water sources: meltwater liberated by the nearby Holden crater impact (continuous deposition over ~10^1–10^2 years), intermittent rainfall or snowmelt during finite periods controlled by orbital evolution (deposition over ~10^4–10^6 years), and highly infrequent runoff or melting of accumulated snowpacks following distant impacts or secular changes in orbital parameters. Local impact-generated runoff and highly infrequent rainfall or snowmelt require unreasonably high and low rates of evaporation, respectively, to maintain the paleolake level. The local impact hypothesis alternatively depends on one flooding episode with very high concentrations of fluvial sediment that are inconsistent with morphologic considerations. Multiple primary impact craters in the area postdate Holden ejecta but were later dissected, indicating fluvial erosion long after the Holden impact. Intermittent rainfall of ~1 cm/day and seasonal snowmelt are both consistent with our results over a deposition timescale totaling ~10^4–10^6 years.
Published by Elsevier B.V.

1. Introduction

1.1. Background

The longstanding debate over the paleoclimate of early Mars has largely focused on warm, wet and cold, dry end-member scenarios, with less consideration of intermediate (cool arid to semiarid) or variable paleoclimates. Valley networks hundreds of kilometers long, valley heads near topographic divides, locally dense dissection, overflowed basins, and a need for aquifer recharge to erode the measured volumes of valleys indicate an active hydrological cycle at times in the past (e.g., Grant, 2000; Craddock and Howard, 2002; Fassett and Head, 2008b; Irwin et al., 2008; Matsubara et al., 2011, 2013). Degradation of impact craters throughout the Noachian Period and into the Hesperian Period required a more effective geomorphic regime than is found currently on Mars (Craddock and Maxwell, 1993; Grant and Schultz, 1993a; Craddock et al., 1997; Forsberg-Taylor et al., 2004; Golombek et al., 2006). The multibasin landscape with numerous impact craters and undissected areas between tributaries is, however, inconsistent with high long-term rates of erosion under sustained humid conditions, relative to Earth (e.g., Pieri, 1980; Carr and Malin, 2000; Irwin et al., 2011).

Meanwhile, a number of paleoclimate modeling studies have found that a thicker CO_2–H_2O atmosphere, which is the simplest extrapolation from the current Mars conditions to those of the ancient past, would not have been able to bring the global mean surface temperature to near 0 °C at the time that the valley networks formed (e.g., Kasting, 1991; Squyres and Kasting, 1994; Haberle, 1998; Colaprete and Toon, 2003; Wordsworth et al., 2013). This discrepancy between empirical and theoretical results has motivated investigations of higher-than-expected solar luminosity, obliquity variations, more effective greenhouse gases, carbon dioxide clouds, albedo differences, and release of volatiles by impacts or volcanism as possible ways of warming the planet (e.g., Baker et al., 1991; Whitmire et al., 1995; Sagan and Chyba, 1997; Segura et al., 2002; Colaprete and Toon, 2003; Segura et al., 2008, 2012; Mischna et al., 2013; Ramirez et al., 2014). Other investigators have examined ways to erode valleys under cold conditions, including ice flow, stream flow under an ice cover, or generation of meltwater

* Corresponding author.
E-mail addresses: irwinr@si.edu (R.P. Irwin), klewis@jhu.edu (K.W. Lewis), ah6p@virginia.edu (A.D. Howard), grantj@si.edu (J.A. Grant).

http://dx.doi.org/10.1016/j.geomorph.2014.10.012
0169-555X/Published by Elsevier B.V.

by surface (impact ejecta) or subsurface (geothermal) heat sources (e.g., Wallace and Sagan, 1979; Carr, 1983; Brakenridge et al., 1985; Wilhelms and Baldwin, 1989; Brakenridge, 1990; Gulick and Baker, 1990; Carr, 1995; Goldspiel and Squyres, 2000; Harrison and Grimm, 2002; Carr and Head, 2003; Mangold et al., 2012a). Quantitative constraints on the Martian paleoclimate based on landform morphometry would have considerable value in guiding these modeling efforts.

The discovery of paleochannels and inverted paleochannels allowed the first empirical constraints on channel-forming (dominant) discharge in past Martian rivers (Malin and Edgett, 2003; Moore et al., 2003; Fassett and Head, 2005; Irwin et al., 2005a; Jaumann et al., 2005). In alluvial channels on Earth, channel-forming discharge is approximately bankfull, controls certain channel dimensions, cumulatively transports more sediment than any other discharge, and has a recurrence interval of a year or two (e.g., Knighton, 1998). The term does not apply to laterally confined bedrock channels or valleys, and it does not imply continuous flow over a prolonged period. Stratigraphic analysis and superimposed crater populations suggest that many of the best preserved fluvial deposits on Mars are Hesperian to Amazonian in age (Grant and Wilson, 2011; Mangold et al., 2012a, 2012b; Irwin and Grant, 2013). The relative youth of these landforms complicates the value for constraining the longer-term paleoclimate, particularly if the Hesperian Period was more like Amazonian (later) than Noachian (earlier) Mars. The Hesperian to Amazonian fluvial deposits have the advantage of better preserved superposition and cross-cutting relationships, as well as smaller superimposed impact craters, which facilitate stratigraphic and chronological interpretations. Impact craters <~2–4 km in diameter are not preserved from the Noachian Period (Hartmann, 2005; Irwin et al., 2013).

The mid-Hesperian or later phases of erosion have been identified in local study areas for some time (e.g., Baker and Partridge, 1986; Grant and Schultz, 1990; Gulick and Baker, 1990), but broader recognition of Hesperian or Amazonian fluvial landforms has improved significantly over the last decade (e.g., Mangold et al., 2004; Quantin et al., 2005; Ansan and Mangold, 2006; Mangold and Ansan, 2006; Mangold et al., 2008; Williams and Malin, 2008; Bouley et al., 2009, 2010; Warner et al., 2010; Grant and Wilson, 2011; Howard and Moore, 2011; Mangold, 2012; Weitz et al., 2013). It remains to be determined whether these late fluvial valleys have a patchy extent or are simply underrecognized, because they are generally less dense than their counterparts from around the Noachian/Hesperian transition. Understanding the local context of relict paleochannels is, therefore, necessary to interpret hydrological implications (if any) on a global scale.

An important contextual relationship is the concentration of large alluvial fans within less-degraded impact craters on Mars (Moore and Howard, 2005; Kraal et al., 2008; Williams and Malin, 2008; Mangold et al., 2012b; Morgan et al., 2014). Local, geologically brief effects of impacts have been implicated for groundwater release, meltwater production, or lake-effect precipitation, which could incise valleys into the crater rim or ejecta (e.g., Newsom et al., 1996; Abramov and Kring, 2005; Morgan and Head, 2009; Barnhart et al., 2010; Harrison et al., 2010; Newsom, 2010; Kite et al., 2011; Mangold et al., 2012a). Global environmental effects have been attributed to larger craters (Segura et al., 2002, 2008; Toon et al., 2010; Segura et al., 2012). Testing the hypothesis that impacts caused significant late fluvial erosion on a local to regional scale, where stratigraphic relationships are best constrained, could have broader implications for impact cratering as an environmental factor on early Mars as well. The key requirement for impact-generated fluvial erosion is its effectiveness over a relatively short geologic timescale, as impact hydrothermal systems can decline over 10^1–10^5 years for craters of 4–100 km in diameter, respectively, or thousands of years for an impact melt sheet 100 m thick (review by Newsom (2010)) (all time intervals in this paper are given in Earth days or years). Interposition of geologically rare or long-lived events between an impact and the end of erosion, or a finding that impact-generated runoff does not explain key fluvial features of a study area, would suggest that impact cratering did not trigger a significant fluvial response at that site. By contrast, fluvial features whose age varies from region to region and that were each concurrent with nearby impact events could support impact cratering as a trigger for fluvial erosion.

Eberswalde crater in Margaritifer Terra (Fig. 1) may provide the best opportunity on Mars to constrain paleohydrology on event, annual, and geologic timescales. The crater is elliptical in shape, 68 by 45 km in diameter, and centered at 24° S, 33.3° W. On the western margin of the crater floor is one of the best preserved fluvial deposits on Mars, with straight and meandering paleochannels that are now expressed in inverted relief (Malin and Edgett, 2003; Moore et al., 2003) (Fig. 2). The crater has no surface outlet, allowing balanced volume calculations on a closed drainage basin. A variety of evidence summarized below suggests that the deposit is a delta, controlled by base levels of standing water in the crater. Eberswalde crater contains other positive-relief stratified deposits that emerge from separate incised valleys around its margin (e.g., Lewis and Aharonson, 2006; Rice et al., 2013), but here we refer to the large western landform as the Eberswalde deposit.

1.2. Purpose

The purpose of this paper is to 1) reexamine the channel-forming discharge and runoff production from the Eberswalde watershed over event flood timescales; 2) consider water supply and loss mechanisms in the paleolake over an annual timescale, for insight into the paleoclimate; and 3) improve upon previous wide-ranging estimates of the longevity of deposition, to constrain the geologic timescale. We evaluate hydrologic parameters using landform morphometry, including the watershed area, contributing valley measurements, geometry of meandering paleochannels, and Eberswalde crater topography. The paleolake water supply and loss must have approximately balanced over the timescales needed for lateral migration of paleochannels under a stable base level, so reasonable rates of evaporation and sediment concentrations inform other key interpretations.

The analyses here allow a discrimination between a continuous flow at a sustained discharge vs. a time-varying or ephemeral discharge for the Eberswalde fluvial system, as well as between short-, medium-, and long-term climate-forcing mechanisms. We examine three hypotheses for the paleohydrology and paleoclimate of Eberswalde crater: 1) short-term, continuous or gradually declining discharge, possibly of meltwater liberated by Holden impact ejecta; 2) a regime with intermittent runoff production, perhaps similar to terrestrial arid to semiarid settings; or 3) highly infrequent runoff production that is more consistent with distant impacts or the evolution of orbital configuration. We contrast published theoretical mechanisms that involve continuous short-term discharge and very high concentrations of sediment with explanations based on empirically derived values of discharge, runoff production, evaporation, and concentration of sediment based on terrestrial fluvial settings. This study provides insight into the Hesperian paleoclimate of Mars and may support planning of a future landed mission. Eberswalde crater was one of four finalist landing sites for the Mars Science Laboratory rover, Curiosity, and much of the work described here was done in support of the landing site selection process.

2. Previous work

2.1. Geologic setting

Eberswalde crater formed about 70 km inside the inner ring of the Early to Middle Noachian, informally named Holden multi-ring impact basin (inner and outer rings of 300 and 600 km in diameter, respectively) (Schultz and Glicken, 1979; Schultz et al., 1982; Irwin and Grant, 2013) (Fig. 1). Early crater degradation at Eberswalde presumably included some rim erosion, wall retreat, and infilling, which are

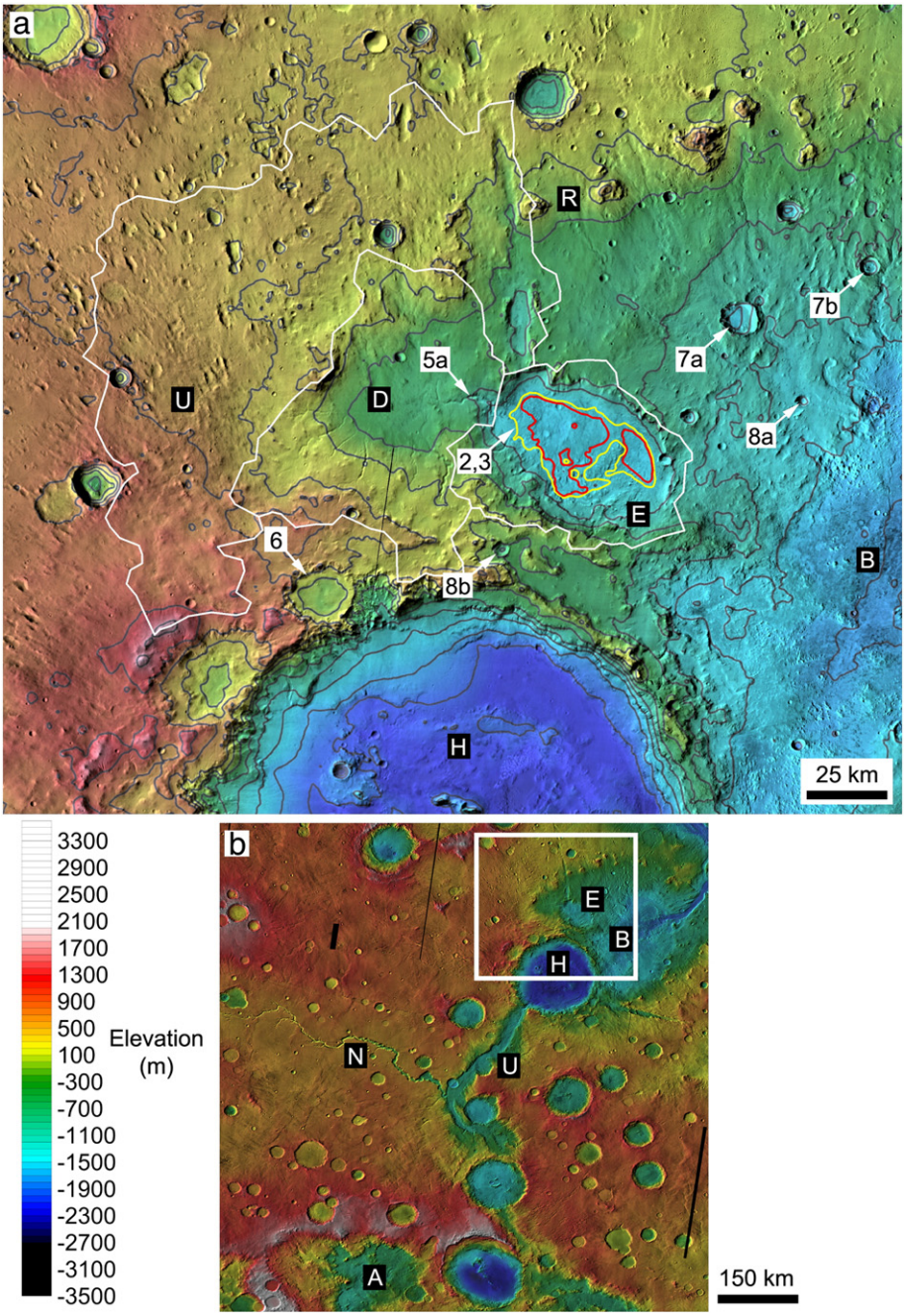

Fig. 1. Context of Eberswalde crater. U: undissected area inside the topographic divide of Eberswalde crater. D: dissected area inside the topographic divide of Eberswalde crater (both U and D would drain through the Eberswalde deposit). E: Eberswalde crater watershed and floor that did not drain through the deposit. B: Holden impact basin (informally named). R: Holden impact basin inner ring. H: Holden crater. U: Uzboi Vallis. N: Nirgal Vallis. A: Argyre impact basin. (a) Eberswalde crater watershed and vicinity. Locations of subsequent figures indicated with arrows. Red line: −1400 m level in Eberswalde crater. Yellow line: −1350 m level. White lines: drainage divides. THEMIS daytime infrared mosaic, 100 m/pixel, colored with MOLA topography (128 pixels/degree), with a contour interval of 350 m. The scene is bounded by 21° S, 26° S, 37° W, and 31° W. (b) Broader regional context, same image base, bounded by 21° S, 37° S, 29° W, and 45° W. White outline is location of Fig. 1a.

typical of Noachian impact craters in equatorial latitudes (Craddock and Maxwell, 1993; Craddock et al., 1997). These craters lack the "terrain softening" or convex-up fringing deposits that suggest ice-facilitated mass wasting in mid-latitude craters to the south (Jankowski and Squyres, 1992, 1993). The elliptical shape of Eberswalde crater could result from a single oblique impact or two contiguous ones with subsequent degradation removing the shared crater rim. Relatively intense (for Mars) fluvial erosion incised valley networks into older geomorphic surfaces across the Martian highlands around the Noachian/Hesperian transition (e.g., Howard et al., 2005; Fassett and Head, 2008a). The current form of the Uzboi–Ladon–Morava Valles mesoscale outflow system also developed at this time (Irwin and Grant, 2013).

During the Hesperian Period, ejecta from Holden crater (26° S, 34° W, 153 km in diameter) partially buried Eberswalde crater and are now exposed over much of its floor (Irwin and Grant, 2013; Rice et al., 2013). Thereafter, the Holden and Eberswalde watersheds shared a drainage divide along the Holden crater rim (Fig. 1a), so any runoff derived from precipitation on that local high should have affected both drainage basins simultaneously. The Holden crater rim also

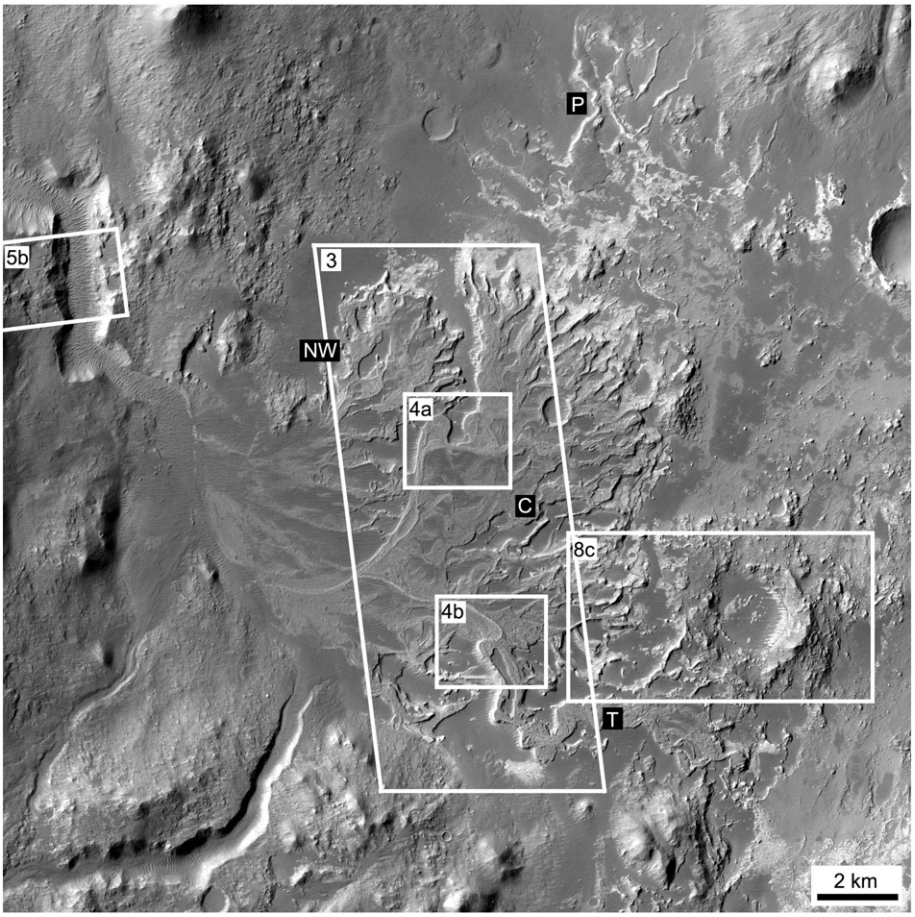

Fig. 2. Eberswalde deposit. NW: northwestern leaf-shaped lobe. C: central leaf-shaped lobe. T: southern tongue-shaped lobe. P: paleochannels that originated from the north rim of the crater, with flow toward the deposit (Lewis and Aharonson, 2006). Locations of subsequent figures are outlined. Note that most paleochannels of the northwestern lobe are not crosscut by the central lobe (Lewis and Aharonson, 2006). CTX image P01_001534_1559.

temporarily dammed Uzboi Vallis, creating an enclosed basin within the valley (Grant et al., 2011) (Fig. 1b).

The amount of time between the Holden impact and the onset of fluvial deposition in Holden and Eberswalde craters is not clear, but we describe relevant observations that suggest a significant time span later in this paper. The oldest exposed infill materials in Holden crater are three members of medium- to fine-grained, phyllosilicate-bearing, light-toned deposits. The uppermost member, which also has the most extensive outcrops, exhibits flat-lying stratification with submeter thickness and lateral continuity over kilometer scales (Grant et al., 2008). Broadly similar deposits are exposed in Uzboi Vallis and may have formed concurrently, when the two basins had no surface connection (Grant et al., 2011).

After at least a hundred meters of light-toned stratigraphy had accumulated on the Holden crater floor, Uzboi Vallis overflowed and incised multiple channels into the southwestern Holden crater wall, most of which were abandoned quickly in favor of a single large entrance breach. The resulting flood partially scoured the light-toned strata and capped them with a coarse to bouldery deposit that radiates in multiple lobes from the Uzboi Vallis breach (Grant and Parker, 2002; Grant et al., 2008, 2011). Flow continued for a limited time afterward, incising an inner valley about 30 km up the Uzboi Vallis floor, but this flow does not appear to have substantially reworked the initial flood deposit as the water level fell in Holden crater (Irwin and Grant, 2013).

In the mid-Hesperian or later, erosion of the western rim of Holden crater, the entire circumference of Ostrov crater to the east, and a number of other deep craters primarily in the 19–30° S latitude band formed large alluvial fans that are less common in older, more degraded Noachian craters (Moore and Howard, 2005; Kraal et al., 2008; Grant and Wilson, 2011, 2012; Mangold et al., 2012b). Early fan-building may have predated the Uzboi flood, contemporary with deposition of the light-toned strata, but it also continued or reactivated afterward, as shown by fan deposits that bury parts of the Uzboi entrance breach (Grant and Wilson, 2012). Along the northwestern side of Holden crater, stratigraphically older alluvial fans have distal escarpments, which may reflect base level control or erosion of fan toes by a lake, and younger fans partly bury these escarpments (Grant and Wilson, 2012). Moreover, floor fractures developed in Holden crater after the Uzboi flood, cross-cutting the bouldery deposit that emanates from Uzboi Vallis, but younger fan materials appear to embay a floor fracture on the southern wall of Holden crater (Irwin and Grant, 2013).

As described below, the architecture of the Eberswalde deposit is consistent with at least two intervals of rising and falling base level (Lewis and Aharonson, 2006; Wood, 2006). These intervals could correspond to fan-building periods in Holden crater, but no evidence supporting a direct link has been reported (the two drainage basins share a drainage divide but not a common drainage network, so any such indications would be indirect). Little to no dissection of the youngest deposit surfaces occurred in Holden and Eberswalde craters during the terminal decline of these drainage basins, so the climate in this region and elsewhere appears to have changed fairly abruptly to the present hyperarid condition (Irwin et al., 2005b).

2.2. Eberswalde deposit morphology

Morphological observations of the Eberswalde deposit favor its origin as a delta and constrain its depositional history. Here we summarize key published observations that inform the analysis in this paper.

Malin and Edgett (2003) and Moore et al. (2003) identified the Eberswalde deposit (Fig. 2) in the Mars Global Surveyor Mars Orbiter Camera (MOC) and the Mars Odyssey Thermal Emission Imaging System (THEMIS) imagery. The three defining features of the deposit are its sinuous ridges with evidence of meander migration and cutoff, a transition from more sinuous proximal ridges to straighter distal ridges, and interfingering of sedimentary strata. Malin and Edgett (2003) interpreted these features as evidence of a progressive or prograding fluvial distributary fan. Aeolian deflation of finer-grained deposits between the paleochannels had formed sinuous ridges, which were capped by more resistant paleochannel deposits. These authors argued that the meander development required long-term, persistent flow, rather than brief, high-magnitude outbursts or low-magnitude discharge of groundwater. They noted at least three gently sloping lobes of the deposit, each of which terminates in an escarpment.

Malin and Edgett (2003) conservatively suggested that this fluvial distributary network may have been a delta, but that this classification was equivocal. Features consistent with the delta interpretation included an abrupt transition from a steeper longitudinal profile of the contributing valley to a lower gradient on the deposit surface, the steep margins of the deposit, the multi-lobate form, and the stratigraphic relationship with rhythmically layered rock on the crater floor. In a concurrent and generally consistent study, Moore et al. (2003) noted that the distributary pattern was consistent with a sediment-dominated delta, rather than one strongly affected by waves or tides. They focused on the fluvial hydrology and timescale of activity as described below.

In contrast, Jerolmack et al. (2004) modeled rapid deposition at Eberswalde of a more extensive alluvial fan, which was subsequently eroded headward to its present dimensions. They noted smaller stratified outcrops in Eberswalde crater east of (and topographically below) the deposit as supporting evidence. Lewis and Aharonson (2006) and Rice et al. (2013) argued that these outcrops were related to independent sediment sources around the crater wall and not directly to the main deposit. For example, small inverted paleochannels that were fed from the northern side of the crater are exposed where the more extensive alluvial fan of Jerolmack et al. (2004) should have been (Fig. 2). Lewis and Aharonson (2006) and Pondrelli et al. (2008a) found it difficult to explain why these paleochannels remained preserved while wind completely removed larger ones supplied from the west. These small, relict paleochannels also suggested that the crater topography had not been strongly modified since deposition (Lewis and Aharonson, 2006), enabling the use of modern topography in the analyses below.

In support of the delta interpretation, Bhattacharya et al. (2005) noted that if the deposit had extended farther into the crater, then its distributary channels should have bifurcated over longer distances. They observed no features that could be attributed to debris flows or sheetfloods, which dominate deposition on many alluvial fans, and they argued that the sinuous channel pattern of the Eberswalde deposit was unlike the braided pattern that is typical of alluvial fans. The common decadal to millennial timescale for lateral migration of meandering paleochannels was inferred to be inconsistent with a very high sedimentation rate, which would have encouraged more frequent avulsions. The development of scroll bars also suggested episodic rather than continuous flooding. Wood (2006) noted many of the same features in support of the delta interpretation, emphasizing the low-gradient lobes with fine-grained floodplains and sinuous paleochannels, as opposed to a steeper, cone-shaped, coarse-grained alluvial fan with straight, radial channels.

Lewis and Aharonson (2006) observed that the large central lobe of the deposit post-dates and advanced in front of the northwestern lobe, without cross-cutting most of the northwestern lobe paleochannels (see also Wood (2006)) (Fig. 2). This observation suggests that the steep margin of the northwestern lobe was a primary (depositional) rather than secondary (erosional) feature, or that the toe of an alluvial fan underwent two separate major retreats, either of which challenges the hypothesis of a short-lived alluvial fan. If the deposit were a delta, then base level control applied at two distinct levels, the second lower than the first. Lewis and Aharonson (2006) used MOC stereo digital elevation models (DEMs) to measure a ~2° average dip of bedding in the distal escarpment of the Eberswalde deposit (all 40 measurements were <6°). They interpreted the exposed stratigraphy as topset rather than foreset bedding, related to aggradation with rising base level rather than progradation into a stable lake. Updated measurements from High-Resolution Imaging Science Experiment (HiRISE) stereo topography give a mean stratigraphic dip of 0.33°, closer to the 0.35° gradient of the deposit surface (Fig. 3). Pondrelli et al. (2008a) also noted mostly shallow dips, with none more than ~6–8°, using High Resolution Stereo Camera (HRSC) data. If this geometry indicates dominantly aggradational growth with limited development of foresets, then the central and northwestern lobes imply two periods of rising base level. The lack of evidence for deep paleochannel downcutting or basinward translation of the shoreline (during the deposition of each lobe) suggested a minimal net loss of lake water during each episode of deposition, and perhaps a long-term relationship between the sediment supply rate and lake level rise.

Wood (2006) published a detailed study of the deposit lobes and paleochannel morphometry. Six lobes were identified based on paleochannel orientation, crosscutting relationships, and downstream location where a transportive paleochannel transitions to distributive architecture. A distinction was made between leaf-shaped (aggradational) and tongue-shaped (degradational and transportive) lobes, suggesting changes in base level during deposition. Pondrelli et al. (2008a) mapped five lobes, and Kargel (2004, p. 238) and Bhattacharya et al. (2005) each mapped four. These four publications and Lewis and Aharonson (2006) all interpreted deposition of the northwestern lobe first, followed by the leaf-shaped central body of the deposit in generally a southeast to northeast progression, and finally up to two narrow, tongue-shaped lobe(s). The latter ones appear to be associated with the two most prominent sinuous paleochannels, which traverse much of the deposit surface basinward before bifurcating into distributary networks.

Subsequent studies of Eberswalde crater have focused on detailed mapping and interpretation of its stratigraphy, including areas topographically below and basinward of the Eberswalde deposit (Pondrelli et al., 2008a, 2008b, 2011; Rice et al., 2013). These maps have larger map scales and contain more units than the 1:1,000,000 map by Irwin and Grant (2013), which differentiates only alluvial and etched units within the crater.

Rice et al. (2013) identified light-toned stratigraphy inside an impact crater that post-dates Holden ejecta on the Eberswalde floor (23.88° S, 33.483°W, 2.4 km diameter), placing a smaller impact event between the Holden impact and the end of fluvial deposition. Pondrelli et al. (2008a) and Rice et al. (2011) interpreted a structural influence on deposition in Eberswalde crater, suggesting that faulting occurred between the Holden impact and subsequent fluvial deposition. Mangold et al. (2012a) interpreted these features as ejecta grooves or faulting related to and coeval with the Holden impact, because they were approximately radial to the larger crater.

Summarizing the observations cited above, the Eberswalde deposit is likely a delta that is composed of mixed sediment, dominated by fine-grained particles and/or sand, but with coarser deposits mostly confined within paleochannels. The medium to fine sediments were susceptible to later aeolian deflation, except where they were armored by coarser or better cemented paleochannel deposits. The leaf-shaped lobes with mostly straight distributaries and a high (proximal) transition to distributive architecture reflect at least two periods of vertical accretion (aggradation). Lateral accretion of coarser paleochannel deposits also occurred at times during deposition, however, generally during periods of stable to falling base level. Extensive delta foresets, which would indicate dominant progradation, have not been identified.

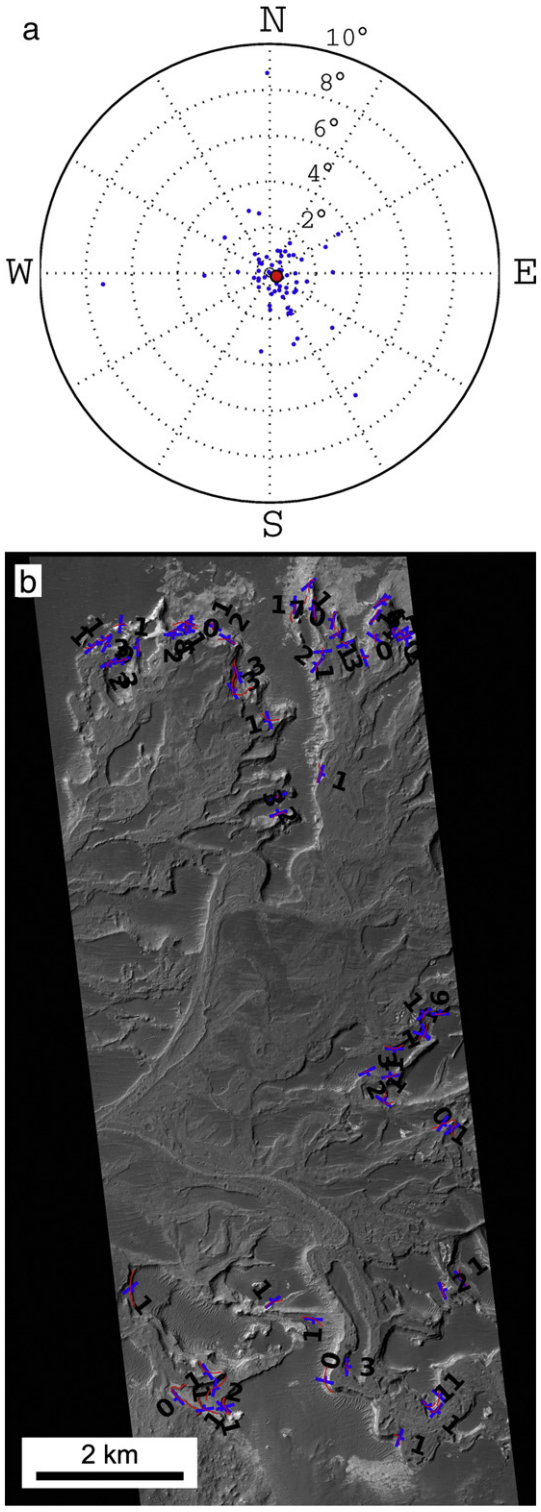

Fig. 3. (a) Compilation of 93 measurements of bedding orientation for individual strata exposed within the Eberswalde deposit (blue). Planar orientations are calculated using linear regression of points extracted from HiRISE stereo topographic data (images PSP_001336_1560/PSP_001534_1560). Error in the regression coefficients is used to estimate angular uncertainty on the vector normal, with all measurements shown having angular errors of less than 2°. The mean orientation of the layers (red) measured at Eberswalde corresponds to a dip of 0.33°, at an azimuth of 24° south of east. (b) Map of the locations of the layers used in this analysis (red), and their corresponding strike and dip.

2.3. Channel-forming discharge

Five studies have estimated either the channel-forming discharge or an instantaneous discharge under assumed flow conditions from the western tributary network to Eberswalde crater, based on paleochannel geometry. These estimates range over less than an order of magnitude, with most converging around several hundred cubic meters per second. The dimensions of the Eberswalde deposit also represent a minimum amount of erosion from the watershed. Table 1 lists the morphometric measurements from prior work, and Table 2 includes variables calculated from these measurements.

Malin and Edgett (2003) made a rough estimate of Eberswalde paleochannel hydrology using the Manning equation (as modified for gravity by Komar (1979)), a Manning roughness coefficient of 0.04, a paleochannel width of 50 m, a flow depth of a few meters, and a gradient of 0.35° (of these values, only the width and gradient were measured). Their estimate of a few hundred cubic meters per second reflects the instantaneous discharge in a channel under these conditions, but it does not imply continuous flow at this level and is not necessarily the channel-forming discharge.

Moore et al. (2003) acknowledged the difficulty in constraining the depth of the paleochannel, so they estimated channel-forming discharge based on empirical relationships with paleochannel geometry, as summarized by Knighton (1987, 1998). Their estimates were 650–975 m^3/s, based on the average meander wavelength of 1858 m, and 300–1600 m^3/s, based on the average width of the paleochannel of 128 m. This range of channel-forming discharge likely resulted in part from the effects of bank strength differences upon channel cross-sectional properties among the various terrestrial sites where the empirical relationships were derived. Similarly, humid–temperate watersheds on Earth with similar size to the Eberswalde watershed have mean annual floods of 300–800 m^3/s. Moore et al. (2003) preferred a channel-forming discharge of 700 m^3/s.

Irwin et al. (2005a) used an empirical relationship between channel width and discharge with a recurrence interval of two years (a proxy for channel-forming discharge), where the relationship is more appropriate for weak channel banks and, therefore, more conservative (Osterkamp and Hedman, 1982). Their estimate was 550 m^3/s, corresponding to runoff production of 1 cm/day, based on measurements of width and contributing area from Moore et al. (2003). Using the gravity scaling guidelines from Irwin et al. (2008), the equivalent channel-forming discharge and runoff production would be ~450 m^3/s and ~0.8 cm/day, respectively.

Jerolmack et al. (2004) used a model for equilibrium shape of channelized alluvial fans (Parker et al., 1998) to obtain a discharge estimate of 280–950 m^3/s for sand transport or 240–790 m^3/s for gravel. Their preferred values were 410 and 340 m^3/s, respectively, very similar to those obtained from the Manning or empirical approaches cited above.

Howard et al. (2007) suggested that some ~1–2 m boulders in the Eberswalde paleochannels were transported clasts rather than weathered blocks of finer-grained fluvial sandstones or conglomerates. They calculated that transport of sparse 1 m boulders down finer-grained channel beds at Eberswalde would be possible at a discharge of ~300–700 m^3/s, if the dimensionless critical shear stress for transport were low (0.01, compared to the more typical value of ~0.047). If boulder transport were frequent, however, then the bed roughness and dimensionless critical shear stress would increase, inhibiting further transport at the gradient of 0.006 measured on the deposit surface.

Bank strength is an important factor in relationships between channel width and channel-forming discharge, as weaker banks typically yield wider channels per unit discharge (e.g., Osterkamp and Hedman, 1982). Moore et al. (2003) noted that bank cohesion was required to support meander development and a prominent chute cutoff on the Eberswalde deposit, but that the source of the cohesion remains unknown (possibilities include cementation, ice, or perhaps

Table 1
Original morphometric measurements from earlier publications. Average values given in parentheses.

Parameter	Malin and Edgett (2003)	Moore et al. (2003)	Jerolmack et al. (2004)	Bhattacharya et al. (2005)	Lewis and Aharonson (2006)	Wood (2006)	Pondrelli et al. (2008a)	Mangold et al. (2012a)
Deposit dimensions (km)	11 × 13	10 × 12, 8 × 11	12.6 long	10 × 25		Lobes vary, some 14–17		
Deposit area (km^2)	115	~100	90			143	138	
Deposit thickness (km)		0.15	<0.15	0.05–0.15	0.1			
Deposit volume (km^3)	6	13.2	6	20–30				5 ± 1
Deposit gradient	<0.0061		0.006					
Channel width (m)	50	112–162 (128)	100			60–240		
Meander wavelength (m)		1018–2866 (1858)						
Max. lake level (m)	−1300	−1200 to −1400			−1400			−1350 to −1400
Lake area (km^2)					240			600
Watershed area (km^2)	4000	4800		4800			6890	5000
Valley volume (km^3)	~24	4.3						

a high clay content). The chute cutoff may indicate variable discharge that occasionally exceeded bankfull, but slow paleochannel aggradation rather than high-magnitude flooding may partly explain the avulsion (Moore et al., 2003), which could have switched the paleochannel back to a former course rather than incising a completely new reach (Jerolmack et al., 2004). Therefore, a large flood may not have been necessary. Irwin et al. (2005b) noted that a discharge of several hundred cubic meters per second is consistent with stream power per unit width at the transition between laterally accreting and braided channel floodplains on Earth (Nanson and Croke, 1992). This discharge predicts fluvial suspension of <3 mm particle sizes that would be susceptible to later aeolian erosion (these particles could be deposited on floodplains during floods and later deflated by wind), whereas coarser clasts of ~3–110 mm would be moved primarily as bed load within the channel. The inferred hydrology was, therefore, consistent with the later relief inversion of the paleochannel. Similarly, Wood (2006) argued that the sinuosity of 1.1–1.8 and the presence of chute rather than neck cutoffs were consistent with a mixed-load channel with relatively low bank cohesion, near the transition between a meandering and braided channel pattern. Two deltaic analogs along the United States Gulf of Mexico coast had a similar distribution of channel width to the Eberswalde deposit, except that the Martian feature lacked the largest distributary channels found in the terrestrial analogs. Wood (2006) speculated that the Eberswalde system lacked the occasional large-scale floods that maintain large distributaries in the terrestrial systems, although the Eberswalde stream was capable of transporting a substantial volume of sediment over time. Occasional intense flooding could have frustrated meander development in this setting, particularly if the bank material were not strongly cohesive.

2.4. Longevity of deposition

In contrast to the relatively well constrained channel-forming discharge, estimates of the deposition timescale have varied over five orders of magnitude. Moore et al. (2003) preferred a timescale of 2000 to 1,000,000 years under Earthlike intermittent flow conditions, but they did not rule out a short timescale resulting from a hypothetical large impact that generated short-term, nearly continuous runoff on a global scale (Segura et al., 2002). Bhattacharya et al. (2005) estimated 150,000 years, based on timescales for meander development and avulsion on Earth.

Assuming continuous input and sufficient loss of water from the crater through infiltration, such that no lake formed, Jerolmack et al. (2004) calculated deposition timescales of 20–70 years for sand or 240–790 years for gravel (preferred timescales of 50 and 340 years, respectively). If the dominant discharge occurred only 5% of the time (18.25 days per year), then formation timescales would be a factor of 20 longer: ~1000 years for sand and ~6800 years for gravel. The peaks of channel-forming floods may last hours rather than weeks per year, however, so the formation timescales could be on the order of 10–100 times their estimate of 1000–6800 years. Similarly, Mangold et al. (2012a) modeled a short formation timescale of years to centuries for the Eberswalde deposit, immediately following and caused by the Holden crater impact. Their model depended on abundant surface or ground ice prior to the impact, heat from the ejecta, and erodible ejecta that could sustain high fluvial water-sediment volume ratios of 3.33 to 100 (ratio of the total water volume that moved through the system to the total volume of deposited sediment).

Lewis and Aharonson (2006) showed that if the Moore et al. (2003) channel-forming discharge of 700 m^3/s were hypothetically continuous

Table 2
Calculated parameters from earlier publications. Best estimates are given in parentheses.

Parameter	Malin and Edgett (2003)	Moore et al. (2003)	Jerolmack et al. (2004)	Bhattacharya et al. (2005)	Irwin et al. (2005a)	Lewis and Aharonson (2006)	Howard et al. (2007)	Mangold et al. (2012a)
Discharge (m^3/s)	~300	650–975, 300–1600 (700)	280–950 (410) sand, 240–790 (340) gravel		550		300–700	
Runoff production, event (cm/day)					1			
Runoff production, total (km^3)			*900 sand, 5000 gravel			200		60–500 (84)
Denudation (m)		<3						
Timescale (y)		2000–1,000,000	50–340 minimum[b]	150,000		~400 minimum		Years to centuries

(this situation is not typical of natural rivers), and losses to evaporation and infiltration were negligible, then the paleolake would accumulate 22 km^3 of water per year and fill to the −1400 m elevation of the deposit surface within 1.2 years. At that rate, a complete flooding of the deposit would take less than 20 years. Malin and Edgett (2003) had also noted that the lake would fill to the −1300 m contour within 20 years if their 300 m^3/s discharge were continuous.

Few investigators have considered water loss from Eberswalde crater as a constraint on their models. Irwin et al. (2005b) offered a limited development of the volume balance argument that is described below. Lewis and Aharonson (2006) estimated that the paleolake was 240 km^2 in area and could lose between 1 and 10 m (0.24 to 2.4 km^3) of water to evaporation per year (these values reflect warm to hot conditions on Earth). At a water-sediment volume ratio of 33 for sand (Jerolmack et al., 2004), a 200 km^3 water supply would be needed to form the deposit, and 24 km^3 of water would remain in the lake, yielding a timescale of ~70–700 years, depending on the rate of evaporation. Lewis and Aharonson (2006), therefore, favored a minimum formation timescale of several hundred years. Mangold et al. (2012a) assumed continuous flow in a closed drainage basin with minimal losses of water to evaporation and infiltration. To keep Eberswalde crater from filling too quickly, their model depended on the high sediment concentrations mentioned above.

Moore et al. (2003) also considered rapid deposition following a hypothetical large impact that affected much of Mars, finding that continuous flow with a 5% sediment concentration by volume could account for the deposit volume within a few years. They noted four complications to the impact-generated flow hypothesis, however: 1) the likely decline in sediment supply as coarse lags developed in the Holden ejecta deposit, 2) the ability to maintain continuous runoff production commensurate with their channel-forming-discharge estimate over a decadal timescale, 3) the low frequency of impacts, and 4) the inconsistent runoff production following impacts of different sizes. The latter two issues would pertain if multiple impacts were responsible, rather than one.

Three previous studies have estimated the total volume of the deposit at ~6 km^3, although larger estimates of 13.2 and 20–30 km^3 have been reported (Table 1 and references therein). The former would imply an average thickness of ~50 m over the deposit area of ~117 km^2 (average of five published area measurements in Table 1). Acknowledging that the deposit thickness is difficult to constrain west of its distal escarpment, which is about 150 m high, we use 6 km^3 for a conservative estimate of the eroded volume. This value corresponds to at least 1 m of areally averaged denudation from the dissected watershed of ~5000 km^2. Malin and Edgett (2003) thought that the volume of the contributing valleys was about four times larger than the 6 km^3 deposit, whereas Moore et al. (2003) interpreted an upland eroded volume of only 4.3 km^3, implying some denudation of inter-valley surfaces in addition to the erosion of valleys.

2.5. Equivocal points in prior literature

Before describing our methods, here we summarize five critical assumptions for the short-duration origin hypotheses that either had little empirical support in prior literature or were directly challenged by other publications. These points are the subjects of the analysis below, in addition to calculations of channel-forming discharge, water mass balance, and formation timescale.

1. Occurrence of ground ice at this location prior to the Hesperian Holden impact (particularly excess rather than pore ice)
2. Continuous flow throughout deposition
3. The ability to sustain high fluvial sediment concentrations from erosion of impact ejecta under a continuous or declining discharge over annual to century timescales
4. A sustainable mechanism for rapid water loss from the basin
5. An originally much more extensive Eberswalde deposit that retreated to its present size

3. Methods

Here we describe methods for estimating channel-forming discharge (event timescale), water input and loss (annual timescale), and the longevity of deposition (geologic timescale). We estimate channel-forming discharge based on empirical relationships with paleochannel geometry (Fig. 4). We then calculate the event rate of runoff production as channel-forming discharge divided by the contributing area of the Eberswalde deposit (Fig. 1a). The annual rate of runoff production is a function of the surface area of a stable paleolake (Fig. 1a), the rate of evaporation, and the contributing area. Finally, we estimate the longevity of deposition as a function of the annual water supply to the paleolake, the sediment concentration, and the deposit volume. We also consider reasonable ranges of parameter values, given the current understanding of the Martian surface, and we compare them to values used in prior work. Finally, we use stratigraphic relationships in the Holden crater vicinity to test our results.

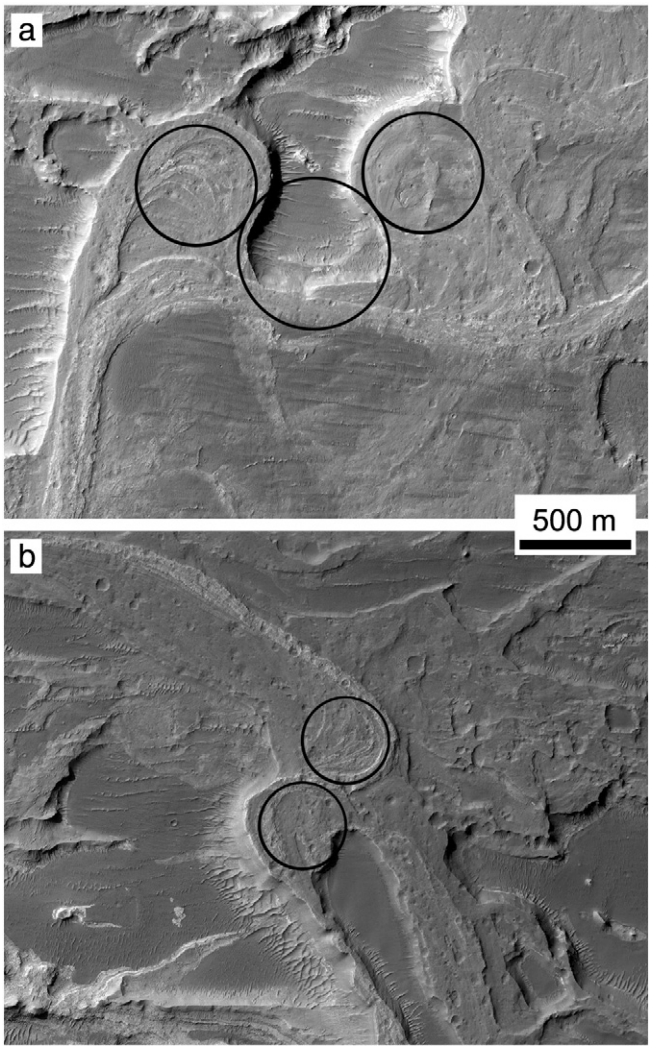

Fig. 4. Meandering inverted paleochannels with evidence of episodic meander development on the Eberswalde deposit. Black circles were drawn for measurements of arc distance and loop radius of curvature. Both images are from HiRISE PSP_001534_1560. See Fig. 2 for locations. (a) Larger northern paleochannel. (b) Smaller southern paleochannel.

3.1. Channel-forming discharge (event timescale)

Alluvial channel form adjusts to a range of discharge that transports the sediment load that the channel receives from outlying surfaces and its own banks. The flow hydrograph is commonly represented by a single channel-forming (dominant) discharge that is bankfull, controls channel dimensions, and cumulatively transports more sediment than any other discharge (e.g., Knighton, 1998). In a U.S. Army Corps of Engineers Technical Note, Copeland et al. (2000, p. 1) defined channel-forming discharge as "a theoretical discharge that if maintained indefinitely would produce the same channel geometry as the natural long-term hydrograph." A channel-forming discharge is not maintained indefinitely in natural rivers, however, even in the largest spring-fed streams in the northwestern United States (Whiting and Stamm, 1995). Continuous flow at some discharge would quickly lead to armoring of a channel bed with clasts that are too coarse to transport. Thereafter, a flow would be mostly clear water, and maintenance of the channel form would depend either on a very small sediment load or on sediment sources that are entirely finer-grained. Otherwise the channel would gradually fill with coarser particles, which rely upon short-term larger floods for transport. Channel-forming discharge can be estimated using field methods as bankfull (the margin of the active floodplain or the level at which the width-depth ratio is a minimum), a specified recurrence interval (typically the mean annual to five-year peak discharge), or effective discharge (which transports the largest fraction of the average annual bed-material load).

These considerations pertain in three ways to the channel-forming discharge of the Eberswalde alluvial paleochannels. First, the paleochannels are assumed to be stable, i.e., adjusted to the channel-forming discharge. Second, the discharge in natural channels can be perennial or ephemeral but is nearly always time-varying, and the higher discharges in a flood hydrograph are critical for the transport and comminution of larger clasts. Third, the channel-forming discharge for a past Martian stream can be estimated only from paleochannel dimensions, but not from measured recurrence interval or sediment transport. Copeland et al. (2000, p. 1) noted that "[f] or channels in arid environments where runoff is generated by localized high-intensity storms and the absence of vegetation ensures that the channel will adjust to each major flood event, the channel-forming discharge concept is generally not applicable." Observations summarized in Section 2.3 above suggest that Eberswalde crater may not have experienced very intense flooding, such as would destroy meander belts and significantly widen channels, but occasional overbank flows are likely and consistent with the channel-forming discharge concept. As Malin and Edgett (2003) noted, the meander loops show that this discharge or range of flows was "persistent" (again without implying a recurrence interval), rather than formed by intense storms or groundwater outbursts.

Empirical relationships between channel-forming discharge and the dimensions of terrestrial alluvial channels can be applied to Mars with a correction for gravity (see review by Irwin et al. (2008)). The Eberswalde inverted distributary network contains two stratigraphically late, meandering paleochannel deposits (which are now cap rocks) with measurable meander dimensions and sharply defined margins (Fig. 4). The width of the paleochannel deposits may reflect some lateral migration of the stream during deposition (i.e., channel fill that is wider than the channel was at any point in time) or narrowing due to backwasting of the margins. Subsequent degradation, however, would not have significantly changed the meander dimensions. For these reasons, meander wavelength is more reliable than width for estimates of paleodischarge in this setting, but it is useful to examine relationships between meander dimensions and width and to estimate paleodischarge using multiple approaches (e.g., Williams et al., 2009).

Williams (1988) listed empirical equations for the dimensions of terrestrial sinuous channels, along with the applicable ranges of the measured independent variables. Bankfull width (W_b) is related to meander wavelength (λ_m), arc distance (λ_a), belt width (B), and loop radius of curvature (R_c) by:

$$W_b = 0.17\lambda_m^{0.89} \quad (1)$$

$$W_b = 0.23\lambda_a^{0.89} \quad (2)$$

$$W_b = 0.27B^{0.89} \quad (3)$$

$$W_b = 0.71R_c^{0.89} \quad (4)$$

All four equations have units of meters. We used Eqs. (1)–(4) to determine what paleochannel width should be for two sets of measured meander dimensions, and we compared the results to width measurements from the same paleochannels based on georeferenced imagery.

Irwin et al. (2005a) estimated a minimum channel-forming discharge (Q, m^3/s) and rate of runoff production for event floods (R_e, discharge divided by contributing area, reported as cm/day) for a set of Martian interior channels, based on width and assuming weak banks. They selected a terrestrial empirical relationship from Osterkamp and Hedman (1982) with relatively low bank strength (and, thus, channels of high width/depth ratio), discharge as the dependent variable, and a recurrence interval of two years (i.e., Q_2, which is commonly associated with channel-forming discharge (Knighton, 1998)). That relationship, when scaled for Martian gravity by a factor of 0.62 (i.e., $0.38^{0.5}$) (Irwin et al., 2008), is:

$$Q_2 = 1.9{W_b}^{1.22}(0.62) = 1.2{W_b}^{1.22}. \quad (5)$$

This equation may underestimate the channel-forming discharge for some meandering rivers, where banks are more cohesive, but it is favored here for its conservative result. Moreover, the boundary shear stress on Mars would be 0.38 times the terrestrial value for given channel dimensions and slope, so simply scaling Eqs. (5) and (6) for gravity does not account for the influences of lower shear stress on channel geometry. The factor of 0.62 is, therefore, an approximation. The discharge with a 1.5-year recurrence interval in the central United States (an approximation of channel-forming discharge for meanders) is related to meander wavelength by (Williams, 1988):

$$Q_{1.5} = 0.011\lambda_m^{1.54}(0.62) = 0.0068\lambda_m^{1.54}. \quad (6)$$

For the two best exposed meandering paleochannels on the Eberswalde deposit, here called the northern and southern paleochannels (Fig. 4), we measured caprock width and meander dimensions on Mars Reconnaissance Orbiter (MRO) Context Camera (CTX) image P01_001534_1559 in transverse Mercator projection. Because of the late stratigraphic position of these paleochannels, our discharge estimates are most applicable to the late depositional history of Eberswalde crater, and the paleohydrology may have been somewhat different in earlier stages. These two meandering paleochannels reflect a transition from distributive to transportive planform with time, perhaps under the influence of a slightly lower base level in the paleolake, such that the stream incised and then migrated laterally through older, weakly cemented deposits (Wood, 2006). It is not clear whether that change in paleochannel morphology was from a reduction in annual runoff production relative to evaporation or sediment supply relative to transport capacity. The surface of the deposit does not appear to have been substantially regraded, however, and both the older northwestern and younger central lobes

of the deposit have a gradient of ~0.006, so our calculations may not differ substantially from long-term conditions.

3.2. Water input and loss (annual timescale)

To maintain a steady lake level over the time needed for meander development during the final stage of deposition at Eberswalde, input of water must balance loss. The input is the sum of base flow, if any, plus event floods whose discharge we approximate by the channel-forming discharge. The runoff production from event floods is defined above. The watershed of Eberswalde crater, including the crater and an intercrater area to the west (Fig. 1a), can be delimited either by topographic divides (e.g., Grant, 1987) or the mapped extent of tributaries seen in imaging. The latter area is smaller and mostly confined within the inner ring of the Early to Middle Noachian Holden impact basin (informally named). Undissected plains that are densely cratered by Hesperian Holden crater secondaries extend north and west of the valley network contributing to Eberswalde. Some of this area lies within the topographic divide but may have contributed little surface water. Moreover, the area that drained into the crater through the Eberswalde deposit (i.e., the contributing area for the inverted paleochannels) is less than the total watershed area by either measure, because small tributaries around the Eberswalde crater rim drained to the crater floor but not to the large deposit (e.g., Lewis and Aharonson, 2006; Rice et al., 2013).

Loss of water to evaporation depends in part on the paleolake area. Its surface can be defined either by the −1350 m base level of the northwestern lobe paleochannels, the −1365 m spillway between the western and eastern sub-basins within the crater, or the −1400 m base level of the central lobe paleochannels. The latter is the most extensive part of the deposit (Fig. 2), suggesting that this level was occupied longer than the others. The area and volume of the basin below those levels have been determined using DEMs (e.g., Lewis and Aharonson, 2006; Mangold et al., 2012a). Given the uncertainties in the various parameters that determine rates of evaporation, we use terrestrial pan rates of evaporation as an upper bound. Paleolake evaporation is about 0.7 of that value (e.g., Dingman, 2002, p. 289), solar insolation at Mars is 0.43 of that at Earth (Kieffer et al., 1992), and a fainter young Sun would further reduce evaporation.

The mean annual rate of runoff production R_a (m/year) is a function of the mean annual rate of evaporation E (m/year), the area of the paleolake A_p (m^2), and the contributing area A_c (m^2):

$$R_a = EA_p/A_c \tag{7}$$

3.3. Longevity of deposition (geologic timescale)

The timescale of deposition T (year) is a function of the deposit volume V_d (m^3), the water-sediment volume ratio V_w/V_s, and the volume of water generated from the watershed and evaporated from the paleolake per year EA_p, where V_w/V_s and EA_p are each averaged over time T:

$$T = V_d(V_w/V_s)/EA_p \tag{8}$$

Assuming that the entire annual water supply (EA_p, reported as m^3/year) passed through the Eberswalde deposit yields a maximum annual rate of runoff production from its limited contributing area, but the timescale for deposition would be conservative for any given water-sediment volume ratio, relative to allowing for additional water sources (e.g., groundwater or Eberswalde rim gullies) that did not add sediment to the deposit. The water-sediment volume ratios used in prior publications have ranged from 3.33 to 100, where the lower end member is a very high density (Mangold et al., 2012a). Jerolmack et al. (2004) used a ratio of 33, which was later applied by Lewis and Aharonson (2006).

In our view, this range of sediment concentration is implausible for the Eberswalde depositional environment, where a more typical water-sediment volume ratio in the range of 1000–10,000 would likely apply. Transport-limited conditions would have prevailed along the Eberswalde deposit paleochannels, which were either slowly aggrading or adjusted to transport the sediment load. The gradient of the deposit at 0.006 or 0.35° (Malin and Edgett, 2003; Jerolmack et al., 2004) in both major lobes is about one sixth that of the contributing valley at 0.034 or 2°. The sudden decline in stream power by a factor of six (or a larger decline in stream power per unit channel width, if the contributing valley had more resistant channel banks) at the deposit head shows that the steep contributing stream was not transporting the maximum sediment load or clast size that it was capable of moving. Otherwise, coarse and abundant sediment would have accumulated at the deposit head, removing the sharp, concave break in slope that now exists at that location. The older northwestern and younger central lobes have a slope break at the head, so these general transport considerations pertained over time, not just during the late-stage flow. Previous investigators have noted the lack of evident debris flows or sheet flood deposits at the site (Bhattacharya et al., 2005). Moreover, rapid channel aggradation from highly concentrated flows would be inconsistent with lateral accretion and meander development, which are observed at multiple geographic and stratigraphic locations on the Eberswalde deposit and require relative stability of the elevation of the channel bed at times.

A lower sediment concentration would also be consistent with the resistant substrate in the Eberswalde watershed. HiRISE images of the contributing area show that Holden crater ejecta have a wide range of particle sizes, including boulders of ~1–10 m in diameter (Mangold et al., 2012a) (Fig. 5). Initial erosion of this material would form an armoring lag, which would thereafter require mechanical or chemical weathering for further incision (Moore et al., 2003). Irwin et al. (2005b) showed that the maximum transportable clast size under normal conditions in the Eberswalde deposit paleochannels was about 0.1 m. Transport of 1 m clasts is only possible under a particular initial condition of low dimensionless critical shear stress and is not sustainable over time (Howard et al., 2007). Most of the sediment had to be <3 mm to be suspended by the channel-forming discharge, deposited on floodplains, and thereafter deflated by wind. Incision of the Eberswalde contributing valleys by tens of meters up to ~200 m, therefore, required a reduction of poorly sorted Holden ejecta to these particle sizes.

The sharp concave break in slope at the deposit head and the paleochannel morphology are, therefore, not consistent with a very high sediment concentration. Empirical constraints are more applicable. The 11 terrestrial rivers that have the highest known average suspended-sediment concentrations and drain to the ocean are mostly in subtropical arid to semiarid regions, where concentrations of 15–45 g/L or water-sediment volume ratios of ~60–180 can occur (Milliman and Farnsworth, 2011, p. 27). These are mostly multithread or incised streams, however, rather than single-thread meandering ones. The other extreme of sediment concentration is four orders of magnitude lower than in these 11 rivers (Milliman and Farnsworth, 2011, p. 27). For these reasons, in the calculations below, we use more typical water-sediment volume ratios in the range of 1000–10,000, i.e., about one to two orders of magnitude below the peak terrestrial values.

Finally, to evaluate possible water sources for the Eberswalde deposit, we examined the ejecta of Holden crater to identify any geologically uncommon or long-lived features, such as primary impact craters that crosscut the ejecta but were later dissected, or stratified deposits that reflect a long depositional history. The identification of such features would suggest that considerable time elapsed between the Holden impact and the end of fluvial

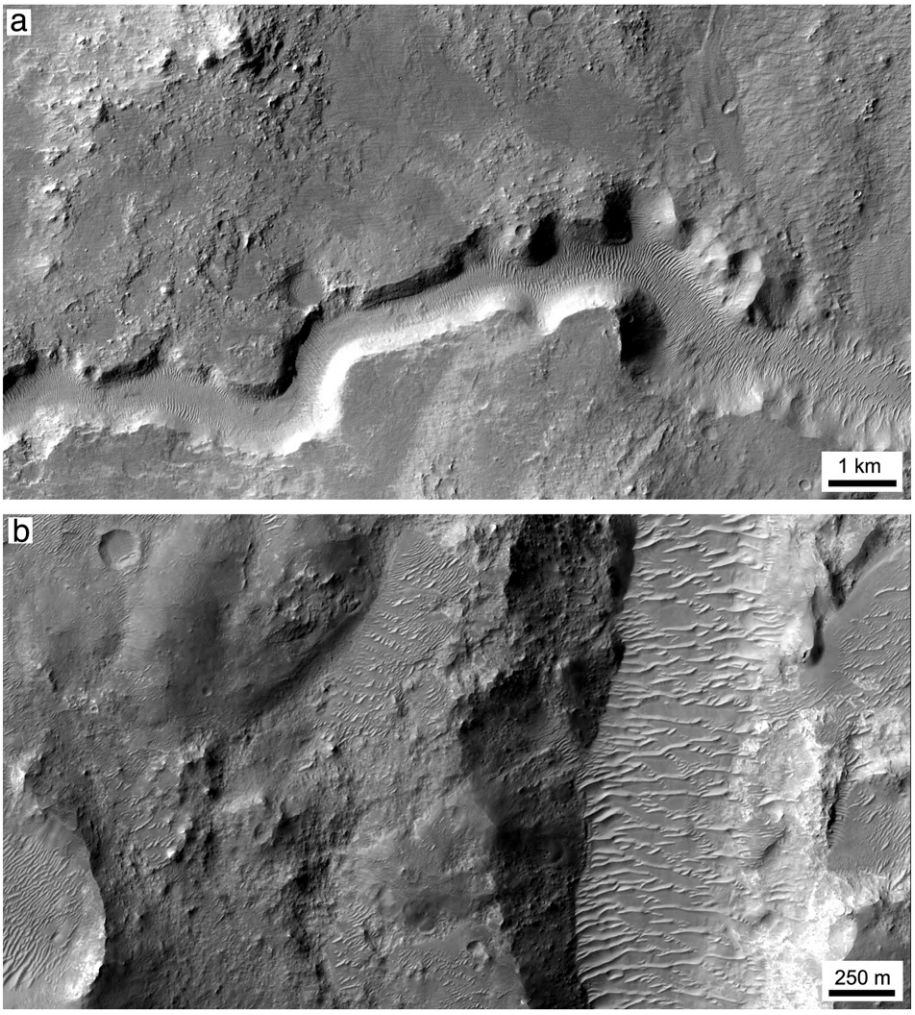

Fig. 5. Bouldery Holden ejecta exposed along the main contributing valley of the Eberswalde deposit. (a) Area centered 12 km northwest and 14 km upstream of the deposit head. Boulders are visible at the 5 m/pixel resolution of the MRO Context Camera. CTX B02_010408_1548. (b) Area centered about 4.7 km upstream of the deposit head. Boulders are visible in valley walls and adjacent surfaces. The valley floor contains later aeolian fill. See Figs. 1 and 2 for locations. HiRISE ESP_028592_1560.

erosion in the area, thereby removing impact heat as the driving factor.

4. Results

4.1. Channel-forming discharge (event timescale)

Table 3 provides the width (mean of five measurements), wavelength, arc distance (mean of two), belt width, and radius of curvature (mean of two) for the northern and southern meandering paleochannels considered in this study. Table 4 shows that the mean of five measured widths closely approximates the expected bankfull widths based on the preserved meander dimensions for both paleochannels (Eqs. (1)–(4)). This similarity gives confidence that either width or meander wavelength can be used to estimate the channel-forming discharge for the two studied paleochannels.

The channel-forming discharge for the northern meandering paleochannel is 450 m^3/s based on Eq. (5) (width) and 400 m^3/s based on Eq. (6) (wavelength), both consistent with prior work (Malin and Edgett, 2003; Moore et al., 2003; Jerolmack et al., 2004; Irwin et al., 2005a; Howard et al., 2007). The results for the southern paleochannel are 140 and 180 m^3/s, respectively. Because of issues with paleochannel width described above, the estimates based on meander wavelength are considered more reliable. Moreover, if we average the width calculated from various meander dimensions (Table 4) and use the result in Eq. (5), then the discharge is within 10 m^3/s of the estimate based on wavelength alone. For the calculations below, we use 400 m^3/s for the northern paleochannel and 200 m^3/s for the southern one, to one significant digit.

These measurements suggest that a lower channel-forming discharge formed the southern paleochannel. If the northern and southern paleochannels were active simultaneously, then the discharge from the contributing area was about 600 m^3/s. If they were not concurrent, then

Table 3
Measurements of meandering inverted paleochannels, rounded to the nearest 10 m.

Paleochannel	Width (mean of 5)	Wavelength	Arc distance (mean of 2)	Belt width	Radius of curvature (mean of 2)
Northern	130	1240	1140	1000	260
Southern	50	740	530	420	170

Table 4
Measured width and calculated width based on meander dimensions in Table 1 and empirical relationships in Eqs. (1)–(4), rounded to the nearest 10 m.

Paleochannel	Measured width (mean of 5)	Width, from wavelength	Width, from arc distance	Width, from belt width	Width, from radius of curvature
Northern	130	100	120	130	100
Southern	50	60	60	60	70

channel-forming discharge (which implies time for channel adjustment and meander development to suit that discharge) varied over the timescale represented by the deposit surface, which is less than the total time of deposition. These differences in paleochannel geometry may reflect changes in the event rate of runoff production toward the end of deposition. As noted by Bhattacharya et al. (2005), the meander loop morphology (Fig. 4) also suggests episodic development with a variable discharge during that time. The stratigraphic relationship between the northern and southern meandering paleochannels is not clear. They appear to split from a common segment upstream, so they may not be far apart in age, but channel associations in inverted systems can be misleading, because of channel entrenchment and aggradation over time (e.g., Williams et al., 2009).

4.2. Water input and loss (annual timescale)

At a channel-forming discharge of 400 m^3/s, the event rate of runoff production for the northern paleochannel was about 2 mm/day from a topographically defined watershed of 17,000 km^2 (not counting the 3000 km^2 of the crater itself) or about 7 mm/day from the 5000 km^2 crossed by visible valleys. Discharge from the dissected area was more likely the major contributor to event floods, although it may include some subsurface flow from a broader area. Terrestrial watersheds typically generate runoff (both Horton and saturation overland flow) unequally across the area (e.g., Betson, 1964), and some precipitation is lost to evaporation and infiltration, so the overall rates of precipitation or melting should have exceeded 1 cm/day at times and would have been locally much higher. For the southern paleochannel, the event rates of runoff production were about half of those determined for the northern one.

The need to maintain the paleolake level at about −1400 m over the timescales of meander development effectively limits annual runoff production over that time. Given the different dimensions of the two paleochannels, we cannot assume a constant discharge over the timescale represented by the deposit surface, but a hypothetical continuous discharge of 300 m^3/s would deliver about 10 km^3/year of water to the paleolake. This volume corresponds to a high rate of 2 to 0.6 m/year of annual runoff production from a watershed of 5000 to 17,000 km^2, respectively. Removing 10 km^3 of water per year would require evaporation of 24 m/year from a 410 km^2 paleolake at the −1400 m level, or 12 m/year from an 810 km^2 paleolake at the −1350 m level. Some water loss to the subsurface is possible, but a net inflow of groundwater is more common than a net outflow in lakes, and fine-grained sedimentation should reduce hypothetical water loss to the subsurface over time.

For comparison, pan rates of evaporation range from ~0.1 m/year in the Canadian Arctic to >3 m/year in the Mojave Desert, California (Kohler et al., 1959; Ferguson et al., 1970; Farnsworth and Thompson, 1982), and they are scaled to open lakes by a factor of 0.7 (Dingman, 2002, p. 289). Reasons exist to favor lower evaporation rates than are found in hot terrestrial deserts. Solar insolation at Mars averages 589 W/m^2 over a Martian year, compared to 1368 W/m^2 for Earth (Kieffer et al., 1992), and at 24° S, insolation is 0.91 of that at the equator at equinox. Energy supplied by a warm contributing river helps little with evaporation from a lake, because the specific heat capacity of water is 4184 J/kg °C, whereas the latent heat is 2,260,000 J/kg. Heat conduction from the ground is typically negligible in lakes (Dingman, 2002, p. 282), and even hot ejecta help little with evaporation (Mangold et al., 2012a). For these reasons, in the calculations below, we use an evaporation rate range of 0.1–1 m/year for Mars.

At the −1400 m level, Lewis and Aharonson (2006) reported a paleolake volume of 24 km^3 based on the Mars Orbiter Laser Altimeter 128 pixel/degree grid, and Mangold et al. (2012a) found 31 km^3 based on HRSC data. Therefore, in the same continuous-flow scenario, filling the lake once to the −1400 m level would take roughly three years. The latter study estimated 66 km^3 below the −1350 m contour, which would correspond to a lake area of ~810 km^2 in the Mars Orbiter Laser Altimeter (MOLA) topography and a filling time closer to seven years.

If the ~6 km^3 Eberswalde deposit were built in the time required to fill the lake once in a continuous-flow regime, then the water-to-sediment volume ratio would be between 4 and 10, depending on the lake volume used. Above we rejected such high sediment concentrations for this site, based on morphological considerations. Moreover, we find at least an order of magnitude difference between discharged water under continuous-flow conditions and possible rates of evaporation if Mars were as hot and arid as many terrestrial deserts. The discrepancy increases to two orders of magnitude in a cold setting. For these reasons, a continuous flow at the channel-forming discharge is not viable at Eberswalde crater.

These considerations yield the range of annual rates of runoff production shown in Table 5. At one end, an early paleolake at −1350 m would require 1.6 to 16 cm of runoff from a 5000 km^2 watershed to offset evaporation of 0.1 to 1 m/year. From the full 17,000 km^2 of the topographically defined watershed, the requirement is 29% of those values. At the −1400 m level, the annual runoff production rate is only 0.82 to 8.2 cm from the 5000 km^2 watershed. The rates of precipitation or melting would be higher during event floods, because of evaporation and infiltration losses from the watershed (e.g., Grant and Schultz, 1993b; Craddock et al., 2012). These annual estimates of runoff production would include any infiltration and groundwater contribution to the paleolake, although groundwater would not add volume to the deposit. A paleolake could be maintained in Eberswalde crater under an arid to semiarid climate, with the channel-forming discharge sustained for less than one day to a few weeks per terrestrial year, depending on the lake level and rate of evaporation.

4.3. Longevity of deposition (geologic timescale)

4.3.1. Estimates of deposition timescale

As described above, the number of years required to build the Eberswalde deposit is a function of the deposit volume, the evaporated volume of water per year, and the average sediment concentration by volume. Table 6 includes the deposition timescales for a range of paleolake levels from −1400 to −1350 m, water-sediment volume ratios from 1000 to 10,000, and evaporation from 0.1 to 1 m/year. For a relatively warm, wet scenario with a larger lake, high evaporation, and abundant sediment supply (the latter is not unique to warm, wet conditions), the timescale is 7000–15,000 (about 10^4) years. In a cold, dry setting with a smaller lake, low evaporation, and low sediment supply, the timescale increases to 700,000–1,500,000 (about 10^6) years. This range is similar to that favored by Moore et al. (2003), if slightly longer. Under intermediate conditions, we would support the ~10^5 year timescale that Bhattacharya et al. (2005) favored based on timescales for meander development and avulsion. The total depth of runoff over these timescales would be ~1–10 km from the 5000 km^2

Table 5
Annual runoff production in the Eberswalde drainage basin for a range of evaporation from a paleolake.

Paleolake level (m)[a]	−1350	−1365	−1400
Paleolake area (km^2)	810	710	410
Evaporated volume (km^3) at 1 m/y [0.1 m/year]	0.81 [0.081]	0.71 [0.071]	0.41 [0.041]
Annual runoff production (cm/year) at 1 m/year [0.1 m/year] evaporation, 5000 km^2 watershed	16 [1.6]	14 [1.4]	8.2 [0.82]
Annual runoff production (cm/year) at 1 m/year [0.1 m/year] evaporation, 17,000 km^2 watershed	4.8 [0.48]	4.2 [0.42]	2.4 [0.24]

[a] These base levels correspond to the northwestern lobe (−1350 m), the spillway between the western and eastern sub-basins within Eberswalde crater (−1365 m), and the central lobes (−1400 m). The crater would overflow at −1000 m but does not appear to have done so.

visually defined watershed or ~0.4–4 km from the 17,000 km^2 topographically defined watershed.

These results are conservative (likely low) for three reasons. First, we assume that the entire paleolake water supply is sediment-laden stream flow rather than clear water or groundwater. Second, in these calculations, all of the water supply for the paleolake passes through the deposit, and none is derived from the rest of the Eberswalde crater rim. Third, we assume that the entire sediment load accumulates on the Eberswalde deposit, and none is transported in suspension farther into the basin or subsequently removed from the deposit by wind. Very high concentrations of sediment in low-gradient channels depend on suspended load, and throughput of a large fraction thereof would add significantly to the Eberswalde deposition timescale for any given sediment concentration (Hoke et al., 2014). Lateral migration of paleochannels also suggests some reworking of sediments on the deposit surface. These considerations would extend the deposition timescale and could largely offset a possible reduction in timescale by reducing the water-sediment volume ratio. The total time of deposition could also be substantially longer if a hiatus in deposition occurred between the northwestern (−1350 m) and central (−1400 m) lobes of the deposit.

4.3.2. Stratigraphic observations near Holden crater

Stratigraphic relationships on the Holden crater ejecta suggest erosive flow long after the Holden impact. The studied paleochannels on the Eberswalde deposit represent late-stage flow, so if they are concurrent with the nearby erosion described below, then they may also substantially post-date Holden crater. The following examples are not exhaustive; Grant and Wilson (2012) identified two of the craters listed below and four other small degraded craters that are superimposed on the Holden rim. Some other craters in the Holden vicinity may also predate the last fluvial erosion, but we have lower confidence in those cases.

Bigbee crater (24.78° S, 34.71° W, 19 km diameter) is located on the western rim of Holden crater, and its rim crosscuts Holden rim structures (Grant and Wilson, 2012) (Fig. 6). This crater was heavily modified internally and externally during the alluvial fan development along the Holden crater rim. Mangold et al. (2012a) argued that Bigbee crater could predate Holden and have survived the impact. Alternatively, they posited that fluvial erosion of the Holden ejecta and deposition at Eberswalde occurred shortly after the Holden impact, but that the Holden fans formed much later and from a different water source, allowing time for Bigbee to form in between. The sharply defined margin of Bigbee crater is not consistent with burial by considerable ejecta (because of its near-rim location), and it does not appear modified by Holden impact structures. We see no reason why a late water source for Holden fans could not have formed the Eberswalde deposit concurrently. Mangold et al. (2012a) also argued that Bigbee crater was a lone example of a dissected crater that could be interpreted to postdate or form along with Holden (e.g., as a binary impactor). We find, however, that the crater is not unique (see also Grant and Wilson (2012)).

Three impact craters that are located northeast of Holden and superimpose Holden ejecta are apparently primary craters with fluvially dissected ejecta. Buta crater (23.233° S, 32.396° W, 11 km in diameter) has valleys that crosscut its ejecta on the eastern and western sides (Fig. 7a). The eastern valley also crosscuts the rims of Holden secondaries at this location 110 km from the Holden crater rim. The other crater (22.953° S, 31.678° W, 145 km from the Holden rim) is 6.1 km in diameter and has dissected ejecta (Fig. 7b). A third fresh crater (23.7° S, 32.05° W, 3.9 km diameter, 99 km from the Holden rim) has dissected ejecta that contains an inverted paleochannel deposit (Fig. 8a). Another fresh crater (24.524° S, 33.727° W, 4.8 km) on the northern part of the Holden rim has ejecta that are buried by deposits emanating from branching valleys on the Holden rim (Fig. 8b).

A small crater on the Eberswalde floor (23.88° S, 33.483° W, 2.4 km diameter) formed into continuous Holden ejecta, 50 km from the Holden rim, but it contains light-toned outcrops similar to those exposed in the Eberswalde deposit (Rice et al., 2013) (Fig. 8c). This is apparently another primary crater that formed between the Holden impact and the end of deposition in Eberswalde.

Table 6
Timescale of deposition for various paleolake levels, mean rates of evaporation (E), and water-sediment volume ratios (V_w/V_s).

Paleolake level (m)[a]	−1350	−1365	−1400
Warm, wet Timescale, $V_w/V_s = 1000$ and $E = 1$ m/year	7000 years	8000 years	15,000 years
Intermediate Timescale, $V_w/V_s = 10{,}000$ and $E = 1$ m/y OR $V_w/V_s = 1000$ and $E = 0.1$ m/year	70,000 years	80,000 years	150,000 years
Cold, dry Timescale, $V_w/V_s = 10{,}000$ and $E = 0.1$ m/year	700,000 years	800,000 years	1,500,000 years

[a] Levels are described in Table 5. The relative sizes of the lobes suggest that the −1400 m level was occupied longer than the others.

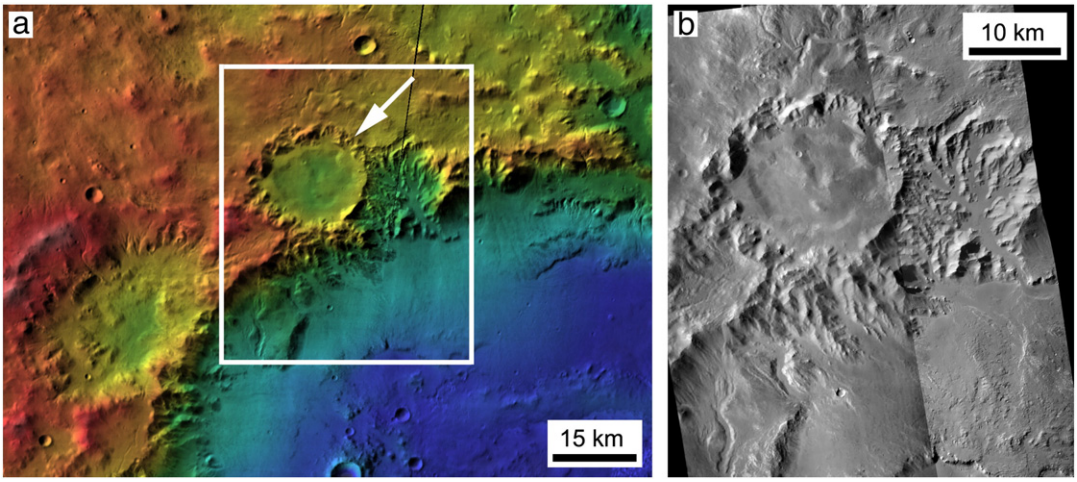

Fig. 6. (a) Bigbee crater (arrow) cross-cuts Holden crater rim structures (24.78° S, 34.71° W, 19 km in diameter). The white outline is the location of Fig. 5b. THEMIS daytime infrared mosaic, 100 m/pixel, colored with MOLA topography as in Fig. 1. (b) Fluvial valleys and alluvial fans southeast of Bigbee lack a mantle of Bigbee crater ejecta, and the Bigbee rim is deeply dissected, thus Bigbee formed before the end of fluvial erosion in the area. The deposits inside Bigbee crater likely formed concurrently with those elsewhere in Holden and Eberswalde craters. Mosaic of CTX P04_002721_1538 and G02_019111_1548.

The Holden rim structures have a morphologically muted appearance compared to those of Gale crater (Fig. 9), which is similar in size and also has preserved secondary chains. The Holden rim appears to have developed a colluvial mantle that was resistant to later aeolian erosion. Despite this muting of the rim structures, the valleys that dissect this mantle are sharply defined, suggesting that slow crater

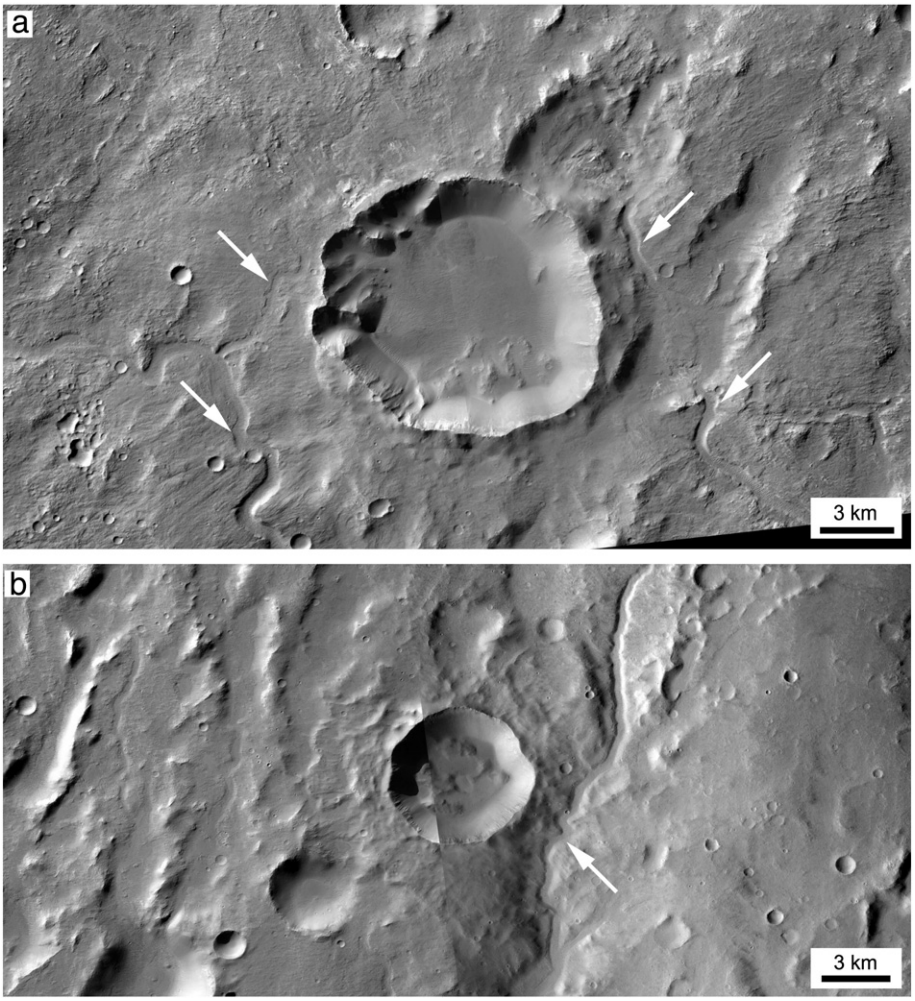

Fig. 7. (a) Buta is a primary crater that partly overlies Holden secondaries to its east (23.233° S, 32.396° W, 11 km in diameter, 110 km from the Holden crater rim). Mosaic of CTX G02_018979_1566 and G23_027260_1580. (b) Unnamed primary crater that superimposes the Holden secondary field, east of Buta (22.953° S, 31.678° W, 6.1 km in diameter, 145 km from the Holden crater rim). See Fig. 1 for locations. Mosaic of CTX P20_008852_1550 and B06_011832_1549. White arrows indicate fluvial valleys that crosscut the crater ejecta in each scene.

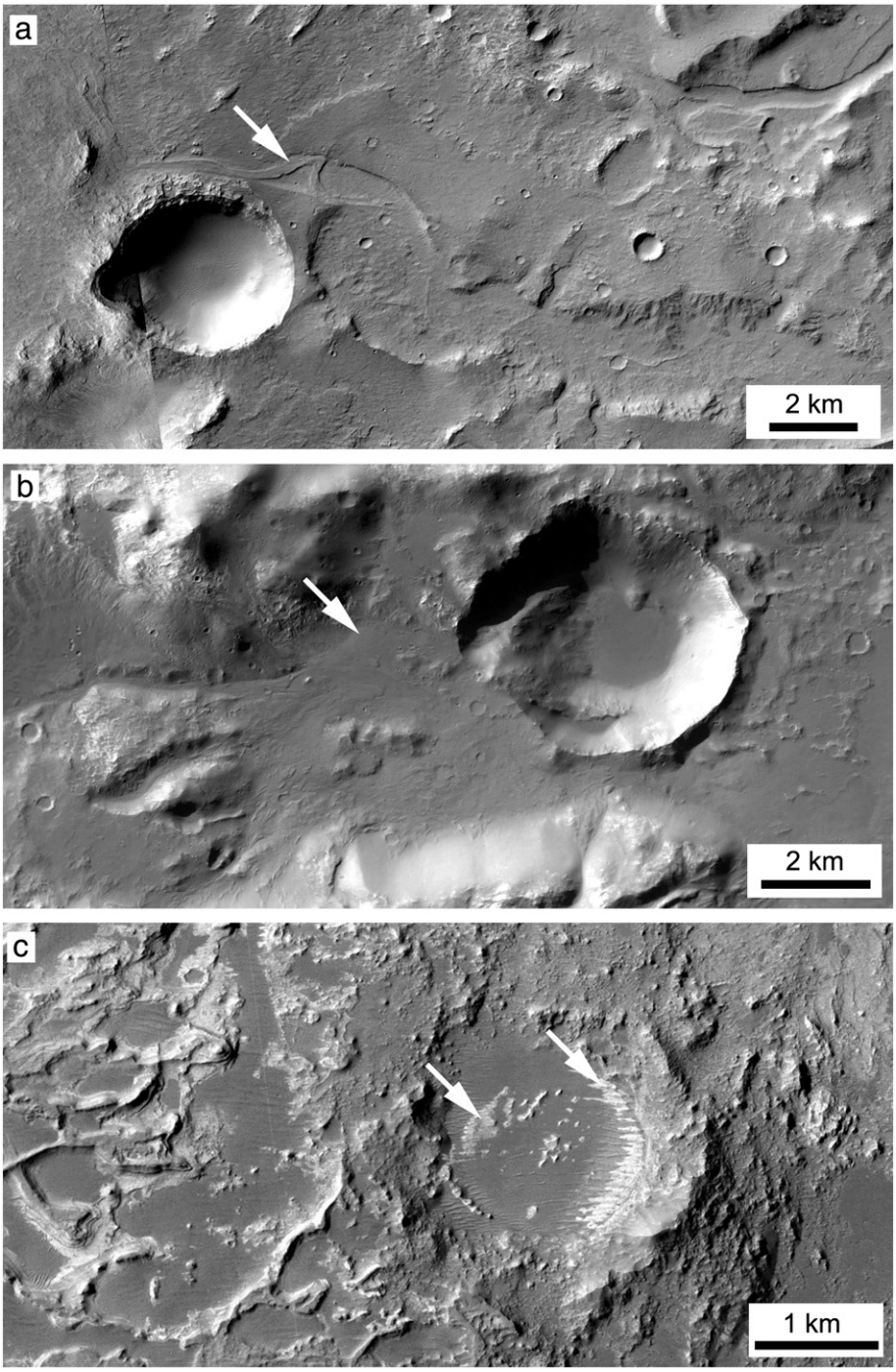

Fig. 8. Post-Holden impact craters with superimposed fluvial deposits. (a) Crater with dissected ejecta and superimposed inverted paleochannel (arrow) (23.7° S, 32.05° W, 3.9 km in diameter, 99 km from the Holden rim). Mosaic of CTX B05_011687_1567 and P20_008852_1550. (b) Crater on the northern part of the Holden rim with ejecta partly buried by deposits (arrow) that emanate from branching valleys (24.524° S, 33.727° W, 4.8 km diameter). CTX B22_018333_1548. (c) Crater on Eberswalde floor containing light-toned materials (23.88° S, 33.483° W, 2.4 km diameter, 50 km from the Holden rim) (Rice et al., 2013). CTX B02_010553_1558. See Figs. 1 and 2 for locations.

modification by various weathering processes, mass wasting, and/or aeolian mantling predated substantial dissection.

Finally, the geologic history of Holden crater involves a complex series of events that are difficult to restrict to a brief period. These events include the deposition of three distinct members of light-toned stratigraphy, flooding of the crater from Uzboi Vallis (whose water sources appear to be independent of Holden crater), and one or two periods of fan-building (e.g., Grant and Parker, 2002; Grant et al., 2008; Irwin and Grant, 2009; Grant et al., 2010; Irwin and Grant, 2013). The fans in northwestern Holden crater have distal escarpments, one of which is partly buried by a later fan, and fan deposition also occurred before and after the Uzboi flood in the southwestern part of the crater (Grant and Wilson, 2012). The older northwestern lobe and younger central lobe of the Eberswalde deposit (Lewis and Aharonson, 2006; Wood, 2006) may correspond to fan-building epochs in Holden crater.

Taken together, these observations suggest that the Hesperian Holden crater was modified in at least two fan-building epochs, punctuated by the Uzboi flood. Significant fluvial erosion outside Holden crater post-dates multiple primary impacts into its ejecta, indicating a substantial gap in time between the Holden impact and one or both

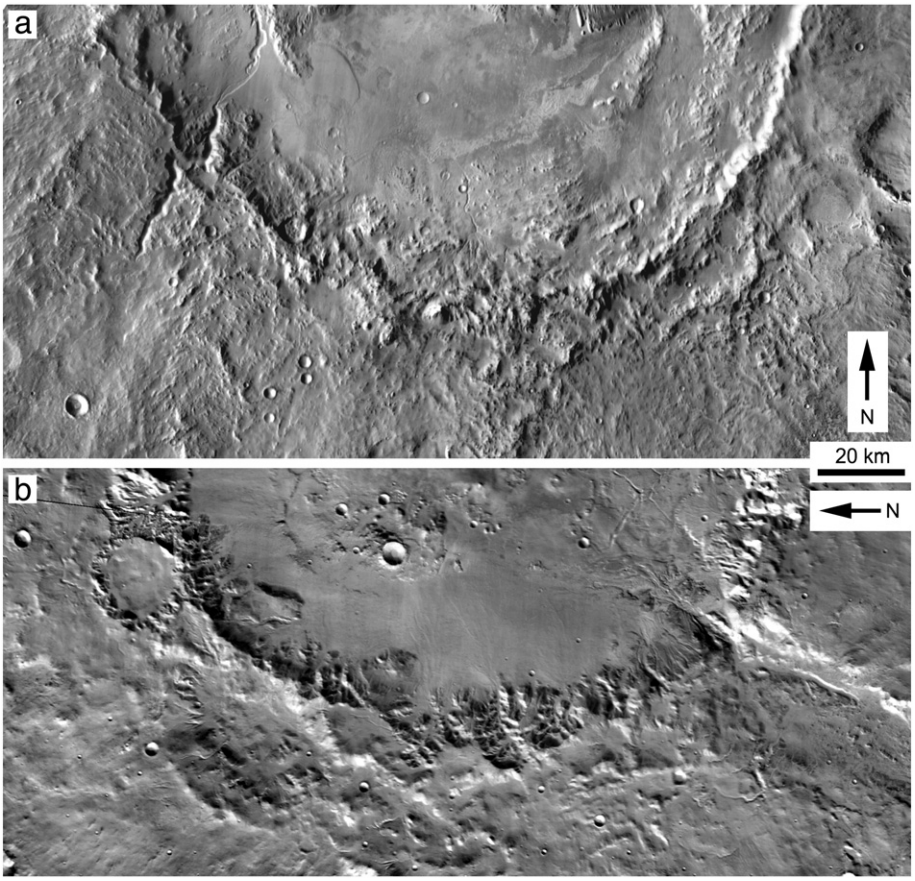

Fig. 9. Comparison of the upslope rim morphology at (a) Gale and (b) Holden craters. Holden rim structures have a relatively muted appearance, but fluvial valleys are sharply defined, suggesting that a more significant colluvial mantle than at Gale developed between the Holden impact and the subsequent dissection. THEMIS daytime infrared mosaic, 100 m/pixel. Fig. 8a is bounded by 5.5° S, 7.25° S, 136° E, and 139.5° E. Fig. 8b is bounded by 24.25° S, 27.75° S, 34.25° W, and 36° W.

erosional epochs. This late fluvial activity should have affected Eberswalde crater along with other surfaces in the vicinity, but Eberswalde records no fluvial erosion after the deposit reached its present extent, so much or all of the Eberswalde deposit likely formed in this late epoch.

5. Discussion and conclusions

Most studies of the paleochannels or stratigraphy of the Eberswalde deposit have favored geologically moderate timescales for deposition (Moore et al., 2003; Bhattacharya et al., 2005; Wood, 2006). Alternatively, Jerolmack et al. (2004) supported groundwater discharge over several decades to centuries, perhaps generated by the Holden crater impact nearby, and Mangold et al. (2012a) further developed a short-lived, impact-generated runoff model related to Holden crater.

As published, the impact-generated runoff model would form the Eberswalde deposit in a geologically brief period of decades to centuries (Jerolmack et al., 2004; Mangold et al., 2012a). However, to do so at a continuous discharge of 300 m^3/s and without raising the paleolake level above −1400 to −1350 m, the model would depend on very low water-sediment volume ratios of 4–10 over a timescale of several years, or rates of evaporation of 12–24 m/year over a longer period, as well as the liberal assumptions discussed in Section 4.3.1. Above we show that high concentrations of fluvial sediment are not plausible for this site, given morphological considerations, and reasonable rates of evaporation for Mars do not allow a continuous discharge into Eberswalde crater while maintaining the paleolake level. The stream discharge in an impact-generated flow would likely decline gradually, absent damming events in the contributing valley (Mangold et al., 2012a), for which we see no supporting evidence. Therefore, the discharge and evaporation requirements would be greater in early stages of flow, relative to the late-stage results that we report here. Evaporation drops under cold conditions, thus, the impact model for Eberswalde paleohydrology is less plausible in the hypothetical cold Hesperian paleoclimate that is one of the main motivations for examining impact-generated runoff.

Highly infrequent runoff production, which might result from multiple distant impacts or slow accumulation of ice and melting over the timescales of orbital and obliquity cycles, is not consistent with the runoff production needed to stabilize the paleolake level against evaporation. If evaporation falls much below ~0.1 m/year, for example in a very cold paleoclimate, then reconciling up to 1 cm/day of event runoff production with $\ll$1 cm/year of annual runoff production and a stable paleolake would require rainfall or snowmelt that is both regular and highly infrequent. Highly infrequent runoff production would likely correspond to a high degree of irregularity in a physically plausible rainfall or snowmelt mechanism, however, making it difficult to maintain the paleolake level. The morphology of the Eberswalde deposit indicates that the paleolake was maintained near −1400 m for at least the timescales needed for paleochannel avulsion and meander development on the deposit surface. We see no evidence for major cut-and-fill cycles on the central lobe of the deposit or for significant advance and retreat of the site of deposition, as would be expected if the lake went dry at more than one interval during deposition (e.g., Cohen, 2003). A distinct ~50 m difference in base level is found between the northwestern and central lobes, likely indicating one major regression during deposition. Although we do not favor event floods with such long recurrence intervals, orbital and obliquity changes and a thicker Hesperian atmosphere

could have facilitated one or more discrete epochs of wetter climate, each with a more Earthlike water cycle, over the total 10^4–10^6 year timescales for deposition in Table 6.

The most plausible scenario includes a narrower range of paleoclimates and timescales of activity. Paleochannel geometry indicates a channel-forming discharge of ~200–400 m^3/s, corresponding to runoff production of 2–7 mm/day at 400 m^3/s and precipitation or rates of melting likely over 1 cm/day at times, if channel-forming floods are sustained over a 24-h period. To balance 0.1–1 m of evaporation per year, no more than one day to a few weeks of continuous flow at the channel-forming discharge are possible, resulting from ~0.2–20 cm of annual runoff production from the watershed. By terrestrial standards, the Eberswalde deposit formed in an arid to possibly semiarid paleoclimate. Using a wide range of evaporation rates that includes the Canadian Arctic allows for seasonal ice covers, which could also help to maintain a lake against evaporation under conditions of low or somewhat less frequent runoff production.

Seasonal runoff production is plausible at Eberswalde. In this scenario, centimeters to perhaps a meter of snow or ice may have accumulated over the Martian winter and melted in the summer (Grant and Wilson, 2012), providing the annual volume and rate of runoff production that we found for Eberswalde crater. Intermittent rainfall or rain-on-snow scenarios are also possible. We do not observe evidence for intense meteorological floods, however, in either Eberswalde (no disproportionately large flood channels or associated deposits (Wood, 2006)) or Holden crater (low-gradient alluvial fan surfaces of gravel to wind-transportable particle sizes rather than resistant debris flows (Moore and Howard, 2005)). Scenarios involving intermittent, moderate rainfall or seasonal snowmelt could limit the flood discharge in a manner that is consistent with deposition of gravel to fine sediment and later development of inverted paleochannels so close to steep source valleys.

The longevity of the Eberswalde paleolake is somewhat harder to constrain, given the additional uncertainty of the average sediment concentration in the contributing stream. The deposit volume of 6 km^3 divided by the dissected contributing area of 5000 km^2 suggests just over 1 m of denudation. Much of this volume came from discrete valleys rather than uniform denudation, however (Malin and Edgett, 2003; Moore et al., 2003). Incision of those valleys up to 100–200 m into bouldery Holden ejecta and production of the <0.1 m particles that could be transported across the Eberswalde deposit under normal flow conditions required preparatory weathering. The 10^4–10^6 year deposition timescales suggested in this study would correspond to a reasonable rate of incision for the contributing valleys of 0.1 to 10 mm per year. The total runoff production from the watershed over the total timescale of deposition would be ~0.3–10 km, and the total precipitation would be higher than these values, because of evaporation and infiltration losses.

The multiple primary impact craters that formed between the Holden impact and the end of fluvial erosion in the area support the findings above by establishing that significant fluvial erosion occurred long after the Holden impact. The key considerations of this study all converge around one or more prolonged periods of late fluvial activity, including a moderate paleohydrology and longevity of deposition at Eberswalde crater. This water cycle would have depended on regional to global climatic factors that were maintained for 10^4–10^6 year periods rather than short-term effects of single or multiple impacts. A hydrological cycle involving precipitation (rain or snow) and surface runoff are indicated, rather than groundwater alone.

Acknowledgments

We credit the Mars Science Laboratory Landing Site Workshops, chaired by John Grant and Matt Golombek, and the related Fluvial Processes Tiger Team for the stimulating discussions that motivated this work, without implying an agreement by all participants in all of the conclusions reported here. We thank Bob Craddock for his insightful discussion and comments on this manuscript prior to submission. Victor Baker and an anonymous reviewer provided very helpful and constructive technical reviews. This work was funded by NASA Mars Data Analysis Program grants NNX10AE64G (Planetary Science Institute) and NNX13AK49G (Smithsonian Institution).

References

Abramov, O., Kring, D.A., 2005. Impact-induced hydrothermal activity on early Mars. J. Geophys. Res. 110, E12S09. http://dx.doi.org/10.1029/2005JE002453.
Ansan, V., Mangold, N., 2006. New observations of Warrego Valles, Mars: evidence for precipitation and surface runoff. Planet. Space Sci. 54, 219–242. http://dx.doi.org/10.1016/j.pss.2005.12.009.
Baker, V.R., Partridge, J.B., 1986. Small Martian valleys: pristine and degraded morphology. J. Geophys. Res. 91 (B3), 3561–3572. http://dx.doi.org/10.1029/JB091iB03p03561.
Baker, V.R., Strom, R.G., Gulick, V.C., Kargel, J.S., Komatsu, G., Kale, V.S., 1991. Ancient oceans, ice sheets and the hydrological cycle on Mars. Nature 352, 589–594. http://dx.doi.org/10.1038/352589a0.
Barnhart, C.J., Nimmo, F., Travis, B.J., 2010. Martian post-impact hydrothermal systems incorporating freezing. Icarus 208, 101–117. http://dx.doi.org/10.1016/j.icarus.2010.01.013.
Betson, R.P., 1964. What is watershed runoff? J. Geophys. Res. 69, 1541–1552.
Bhattacharya, J.P., Payenberg, T.H.D., Lang, S.C., Bourke, M., 2005. Dynamic river channels suggest a long-lived Noachian crater lake on Mars. Geophys. Res. Lett. 32, L10201. http://dx.doi.org/10.1029/2005GL022747.
Bouley, S., Ansan, V., Mangold, N., Masson, Ph., Neukum, G., 2009. Fluvial morphology of Naktong Vallis, Mars: a late activity with multiple processes. Planet. Space Sci. 57, 982–999. http://dx.doi.org/10.1016/j.pss.2009.01.015.
Bouley, S., Craddock, R.A., Mangold, N., Ansan, V., 2010. Characterization of fluvial activity in Parana Valles using different age-dating techniques. Icarus 207, 686–698. http://dx.doi.org/10.1016/j.icarus.2009.12.030.
Brakenridge, G.R., 1990. The origin of fluvial valleys and early geologic history, Aeolis quadrangle, Mars. J. Geophys. Res. 95, 17,289–17,308. http://dx.doi.org/10.1029/JB095iB11p17289.
Brakenridge, G.R., Newsom, H.E., Baker, V.C., 1985. Ancient hot springs on Mars: origins and paleoenvironmental significance of small Martian valleys. Geology 13, 859–862. http://dx.doi.org/10.1130/0091-7613(1985)13<859:AHSOMO>2.0.CO;2.
Carr, M.H., 1983. Stability of streams and lakes on Mars. Icarus 56, 476–495.
Carr, M.H., 1995. The Martian drainage system and the origin of valley networks and fretted channels. J. Geophys. Res. 100, 7479–7507.
Carr, M.H., Head III, J.W., 2003. Basal melting of snow on early Mars: a possible origin of some valley networks. Geophys. Res. Lett. 30 (24), 2245. http://dx.doi.org/10.1029/2003GL018575.
Carr, M.H., Malin, M.C., 2000. Meter-scale characteristics of Martian channels and valleys. Icarus 146, 366–386. http://dx.doi.org/10.1006/icar.2000.6428.
Cohen, A.S., 2003. Paleolimnology: The History and Evolution of Lake Systems. Oxford Univ. Press, New York.
Colaprete, A., Toon, O.B., 2003. Carbon dioxide clouds in an early dense Martian atmosphere. J. Geophys. Res. 108 (E4), 5025. http://dx.doi.org/10.1029/2002JE001967.
Copeland, R.R., Biedenharn, D.S., Fischenich, J.C., 2000. Channel-forming discharge. U.S. Army Corps of Engineers Technical Note ERDC/CHL CHETN-VIII-5.
Craddock, R.A., Howard, A.D., 2002. The case for rainfall on a warm, wet early Mars. J. Geophys. Res. 107 (E11), 5111. http://dx.doi.org/10.1029/2001JE001505.
Craddock, R.A., Maxwell, T.A., 1993. Geomorphic evolution of the Martian highlands through ancient fluvial processes. J. Geophys. Res. 98, 3453–3468. http://dx.doi.org/10.1029/92JE02508.
Craddock, R.A., Maxwell, T.A., Howard, A.D., 1997. Crater morphometry and modification in the Sinus Sabaeus and Margaritifer Sinus regions of Mars. J. Geophys. Res. 102, 13,321–13,340. http://dx.doi.org/10.1029/97JE01084.
Craddock, R.A., Howard, A.D., Irwin III, R.P., Tooth, S., Williams, R.M.E., Chu, P.-S., 2012. Drainage network development in the Keanakāko'i tephra, Kīlauea Volcano, Hawai'i: implications for fluvial erosion and valley network formation on early Mars. J. Geophys. Res. 117, E08009. http://dx.doi.org/10.1029/2012JE004074.
Dingman, S.L., 2002. Physical Hydrology, Second edition. Prentice Hall, Upper Saddle River, New Jersey.
Farnsworth, R.K., Thompson, E.S., 1982. Mean monthly, seasonal, and annual pan evaporation rates for the United States. National Oceanic and Atmospheric Administration Technical Report, National Weather Service 34.
Fassett, C.I., Head III, J.W., 2005. Fluvial sedimentary deposits on Mars: ancient deltas in a crater lake in the Nili Fossae region. Geophys. Res. Lett. 32, L14201. http://dx.doi.org/10.1029/2005GL023456.
Fassett, C.I., Head III, J.W., 2008a. The timing of Martian valley network activity: constraints from buffered crater counting. Icarus 195, 61–89. http://dx.doi.org/10.1016/j.icarus.2007.12.009.
Fassett, C.I., Head III, J.W., 2008b. Valley network-fed, open-basin lakes on Mars: distribution and implications for Noachian surface and subsurface hydrology. Icarus 198, 37–56. http://dx.doi.org/10.1016/j.icarus.2008.06.016.
Ferguson, H.L., O'Neill, A.D.J., Cork, H.F., 1970. Mean evaporation over Canada. Water Resour. Res. 6 (6), 1618–1633.
Forsberg-Taylor, N.K., Howard, A.D., Craddock, R.A., 2004. Crater degradation in the Martian highlands: morphometric analysis of the Sinus Sabaeus region and simulation modeling suggest fluvial processes. J. Geophys. Res. 109, E05002. http://dx.doi.org/10.1029/2004JE002242.

Goldspiel, J.M., Squyres, S.W., 2000. Groundwater sapping and valley formation on Mars. Icarus 148, 176–192. http://dx.doi.org/10.1006/icar.2000.6465.
Golombek, M.P., Grant, J.A., Crumpler, L.S., Greeley, R., Arvidson, R.E., Bell III, J.F., Weitz, C.M., Sullivan, R., Christensen, P.R., Soderblom, L.A., Squyres, S.W., 2006. Erosion rates at the Mars Exploration Rover landing sites and long-term climate change on Mars. J. Geophys. Res. 111, E12S10. http://dx.doi.org/10.1029/2006JE002754.
Grant, J.A., 1987. The geomorphic evolution of eastern Margaritifer Sinus, Mars. Advances in Planetary Geology. NASA/TM 89871, pp. 1–268.
Grant, J.A., 2000. Valley formation in Margaritifer Sinus, Mars, by precipitation-recharged ground-water sapping. Geology 28, 223–226. http://dx.doi.org/10.1130/0091-7613(2000)28<223:VFIMSM>2.0.CO;2.
Grant, J.A., Parker, T.J., 2002. Drainage evolution in the Margaritifer Sinus region, Mars. J. Geophys. Res. 107 (E9), 5066. http://dx.doi.org/10.1029/2001JE001678.
Grant, J.A., Schultz, P.H., 1990. Gradational epochs on Mars: evidence from west-northwest of Isidis basin and Electris. Icarus 84, 166–195.
Grant, J.A., Schultz, P.H., 1993a. Degradation of selected terrestrial and Martian impact craters. J. Geophys. Res. 98, 11,025–11,042. http://dx.doi.org/10.1029/93JE00121.
Grant, J.A., Schultz, P.H., 1993b. Erosion of ejecta at Meteor Crater, Arizona. J. Geophys. Res. 98, 15,033–15,047. http://dx.doi.org/10.1029/93JE01580.
Grant, J.A., Wilson, S.A., 2011. Late alluvial fan formation in southern Margaritifer Terra, Mars. Geophys. Res. Lett. L08201 http://dx.doi.org/10.1029/2011GL046844.
Grant, J.A., Wilson, S.A., 2012. A possible synoptic source of water for alluvial fan formation in southern Margaritifer Terra, Mars. Planet. Space Sci. 72, 44–52. http://dx.doi.org/10.1016/j.pss.2012.05.020.
Grant, J.A., Irwin III, R.P., Grotzinger, J.P., Milliken, R.E., Tornabene, L.L., McEwen, A.S., Weitz, C.M., Squyres, S.W., Glotch, T.D., Thomson, B.J., 2008. HiRISE imaging of impact megabreccia and sub-meter aqueous strata in Holden crater, Mars. Geology 36, 195–198. http://dx.doi.org/10.1130/G24340A.1.
Grant, J.A., Irwin III, R.P., Wilson, S.A., 2010. Aqueous depositional settings in Holden crater, Mars. In: Cabrol, N.A., Grin, E.A. (Eds.), Lakes on Mars. Elsevier, Oxford, U.K., pp. 323–346. http://dx.doi.org/10.1016/B978-0-444-52854-4.00012-X.
Grant, J.A., Irwin III, R.P., Wilson, S.A., Buczkowski, D., Siebach, K., 2011. A lake in Uzboi Vallis and implications for late Noachian–Early Hesperian climate on Mars. Icarus 212, 110–122. http://dx.doi.org/10.1016/j.icarus.2010.11.024.
Gulick, V.C., Baker, V.R., 1990. Origin and evolution of valleys on Martian volcanoes. J. Geophys. Res. 95, 14,325–14,344. http://dx.doi.org/10.1029/JB095iB09p14325.
Haberle, R.M., 1998. Early Mars climate models. J. Geophys. Res. 103, 28,467–28,479. http://dx.doi.org/10.1029/98JE01396.
Harrison, K.P., Grimm, R.E., 2002. Controls on Martian hydrothermal systems: application to valley network and magnetic anomaly formation. J. Geophys. Res. 107 (E5), 5025. http://dx.doi.org/10.1029/2001JE001616.
Harrison, T.N., Malin, M.C., Edgett, K.S., Shean, D.E., Kennedy, M.R., Lipkaman, L.J., Cantor, B.A., Posiolova, L.V., 2010. Impact-induced overland fluid flow and channelized erosion at Lyot Crater, Mars. Geophys. Res. Lett. 37, L21201. http://dx.doi.org/10.1029/2010GL045074.
Hartmann, W.K., 2005. Martian cratering 8: isochron refinement and the chronology of Mars. Icarus 174, 294–320. http://dx.doi.org/10.1016/j.icarus.2004.11.023.
Hoke, M.R.T., Hynek, B.M., Di Achille, G., Hutton, E.W.H., 2014. The effects of sediment supply and concentrations on the formation timescale of Martian deltas. Icarus 228, 1–12. http://dx.doi.org/10.1016/j.icarus.2013.09.017.
Howard, A.D., Moore, J.M., 2011. Late Hesperian to Early Amazonian midlatitude Martian valleys: evidence from Newton and Gorgonum basins. J. Geophys. Res. 116, E05003. http://dx.doi.org/10.1029/2010JE003782.
Howard, A.D., Moore, J.M., Irwin III, R.P., 2005. An intense terminal epoch of widespread fluvial activity on early Mars: 1. Valley network incision and associated deposits. J. Geophys. Res. 110, E12S14. http://dx.doi.org/10.1029/2005JE002459.
Howard, A.D., Moore, J.M., Irwin III, R.P., Dietrich, W.E., 2007. Boulder transport across the Eberswalde delta. Lunar Planet. Sci. Conf. 38. Lunar and Planetary Institute, Houston, Texas (abstract 1168).
Irwin, R.P., III, Grant, J.A., 2013. Geologic map of MTM −15027, −20027, −25027, and −25032 quadrangles, Margaritifer Terra region of Mars. U.S. Geol. Surv. Sci. Inv. Map 3209, scale 1:1,000,000.
Irwin III, R.P., Craddock, R.A., Howard, A.D., 2005a. Interior channels in Martian valley networks: discharge and runoff production. Geology 33 (6), 489–492. http://dx.doi.org/10.1130/G21333.1.
Irwin III, R.P., Howard, A.D., Craddock, R.A., Moore, J.M., 2005b. An intense terminal epoch of widespread fluvial activity on early Mars: 2. Increased runoff and paleolake development. J. Geophys. Res. 110, E12S15. http://dx.doi.org/10.1029/2005JE002460.
Irwin III, R.P., Howard, A.D., Craddock, R.A., 2008. Fluvial valley networks on Mars. In: Rice, S., Roy, A., Rhoads, B. (Eds.), River Confluences, Tributaries, and the Fluvial Network. John Wiley, West Sussex, U.K., pp. 409–430.
Irwin III, R.P., Grant, J.A., 2009. Large basin overflow floods on Mars. In: Burr, D.M., Baker, V.R., Carling, P.A. (Eds.), Megaflooding on Earth and Mars. Cambridge University Press, Cambridge, UK, pp. 209–224.
Irwin III, R.P., Craddock, R.A., Howard, A.D., Flemming, H.L., 2011. Topographic influences on development of Martian valley networks. J. Geophys. Res. 116, E02005. http://dx.doi.org/10.1029/2010JE003620.
Irwin III, R.P., Tanaka, K.L., Robbins, S.J., 2013. Distribution of Early, Middle, and Late Noachian cratered surfaces in the Martian highlands: implications for resurfacing events and processes. J. Geophys. Res. Planets 118, 278–291. http://dx.doi.org/10.1002/jgre.20053.
Jankowski, D.G., Squyres, S.W., 1992. The topography of impact craters in "softened" terrain on Mars. Icarus 100, 26–39.
Jankowski, D.G., Squyres, S.W., 1993. "Softened" impact craters on Mars: implications for ground ice and the structure of the Martian regolith. Icarus 106, 365–379.
Jaumann, R., Reiss, D., Frei, S., Neukum, G., Scholten, F., Gwinner, K., Roatsch, T., Matz, K.-D., Mertens, V., Hauber, E., Hoffmann, H., Köhler, U., Head, J.W., Hiesinger, H., Carr, M.H., 2005. Interior channels in Martian valleys: constraints on fluvial erosion by measurements of the Mars Express High Resolution Stereo Camera. Geophys. Res. Lett. 32, L16203. http://dx.doi.org/10.1029/2005GL023415.
Jerolmack, D.J., Mohrig, D., Zuber, M.T., Byrne, S., 2004. A minimum time for the formation of Holden Northeast fan, Mars. Geophys. Res. Lett. 31, L21701. http://dx.doi.org/10.1029/2004GL021326.
Kargel, J.S., 2004. Mars — A warmer, wetter planet. Springer-Praxis, Chichester, U.K.
Kasting, J.F., 1991. CO_2 condensation and the climate of early Mars. Icarus 62, 175–190.
Kieffer, H.H., Jakosky, B.M., Snyder, C.W., 1992. The planet Mars: from antiquity to the present. In: Kieffer, H.H., Jakosky, B.M., Snyder, C.W., Matthews, M.S. (Eds.), Mars. University of Arizona Press, Tucson, AZ, pp. 1–33.
Kite, E.S., Michaels, T.I., Rafkin, S., Manga, M., Dietrich, W.E., 2011. Localized precipitation and runoff on Mars. J. Geophys. Res. 116, E07002. http://dx.doi.org/10.1029/2010JE003783.
Knighton, A.D., 1987. River channel adjustment — the downstream dimension. In: Richards, K.S. (Ed.), River Channels: Environment and Process. Basil Blackwell Ltd., Oxford, U.K., pp. 95–128.
Knighton, A.D., 1998. Fluvial Forms and Processes: A New Perspective. Arnold, London.
Kohler, M.A., Nordenson, T.J., Baker, D.R., 1959. Evaporation maps for the United States. U.S. Department of Commerce, Weather Bureau, Technical Paper 37. U.S. Government Printing Office, Washington D.C.
Komar, P.D., 1979. Comparisons of the hydraulics of water flows in Martian outflow channels with flows of similar scale on Earth. Icarus 37, 156–181.
Kraal, E.R., Asphaug, E., Moore, J.M., Howard, A., Bredt, A., 2008. Catalogue of large alluvial fans in Martian impact craters. Icarus 194, 101–110. http://dx.doi.org/10.1016/j.icarus.2007.09.028.
Lewis, K.W., Aharonson, O., 2006. Stratigraphic analysis of the distributary fan in Eberswalde crater using stereo imagery. J. Geophys. Res. 111, E06001. http://dx.doi.org/10.1029/2005JE002558.
Malin, M.C., Edgett, K.S., 2003. Evidence for persistent flow and aqueous sedimentation on early Mars. Science 302, 1931–1934. http://dx.doi.org/10.1126/science.1090544.
Mangold, N., 2012. Fluvial landforms on fresh impact ejecta on Mars. Planet. Space Sci. 62, 69–85. http://dx.doi.org/10.1016/j.pss.2011.12.009.
Mangold, N., Ansan, V., 2006. Detailed study of an hydrological system of valleys, a delta and lakes in the Southwest Thaumasia region, Mars. Icarus 180, 75–87. http://dx.doi.org/10.1016/j.icarus.2005.08.017.
Mangold, N., Quantin, C., Ansan, V., Delacourt, C., Allemand, P., 2004. Evidence for precipitation on Mars from dendritic valleys in the Valles Marineris area. Science 305, 78–81. http://dx.doi.org/10.1126/science.1097549.
Mangold, N., Ansan, V., Masson, Ph., Quantin, C., Neukum, G., 2008. Geomorphic study of fluvial landforms on the northern Valles Marineris plateau, Mars. J. Geophys. Res. 113, E08009. http://dx.doi.org/10.1029/2007JE002985.
Mangold, N., Kite, E.S., Kleinhans, M.G., Newsom, H., Ansan, V., Hauber, E., Kraal, E., Quantin, C., Tanaka, K., 2012a. The origin and timing of fluvial activity at Eberswalde crater, Mars. Icarus 220, 530–551. http://dx.doi.org/10.1016/j.icarus.2012.05.026.
Mangold, N., Adeli, S., Conway, S., Ansan, V., Langlais, B., 2012b. A chronology of early Mars climatic evolution from impact crater degradation. J. Geophys. Res. 117, E04003. http://dx.doi.org/10.1029/2011JE004005.
Matsubara, Y., Howard, A.D., Drummond, S.A., 2011. Hydrology of early Mars: lake basins. J. Geophys. Res. 116, E04001. http://dx.doi.org/10.1029/2010JE003739.
Matsubara, Y., Howard, A.D., Gochenour, J.P., 2013. Hydrology of early Mars: valley network incision. J. Geophys. Res. Planets 118. http://dx.doi.org/10.1002/jgre.20081.
Milliman, J.D., Farnsworth, K.L., 2011. River Discharge to the Coastal Ocean: A Global Synthesis. Cambridge University Press, Cambridge, U.K.
Mischna, M., Baker, V., Milliken, R., Richardson, M., Lee, C., 2013. Effects of obliquity and water vapor/trace gas greenhouses in the early Martian climate. J. Geophys. Res. 118, 560–576. http://dx.doi.org/10.1002/jgre.20054.
Moore, J.M., Howard, A.D., 2005. Large alluvial fans on Mars. J. Geophys. Res. 110, E04005. http://dx.doi.org/10.1029/2004JE002352.
Moore, J.M., Howard, A.D., Dietrich, W.E., Schenk, P.M., 2003. Martian layered fluvial deposits: implications for Noachian climate scenarios. Geophys. Res. Lett. 30 (24), 2292. http://dx.doi.org/10.1029/2003GL019002.
Morgan, G.A., Head III, J.W., 2009. Sinton crater, Mars: evidence for impact into a plateau icefield and melting to produce valley networks at the Hesperian–Amazonian boundary. Icarus 202, 39–59. http://dx.doi.org/10.1016/j.icarus.2009.02.025.
Morgan, A.M., Howard, A.D., Hobley, D.E.J., Moore, J.M., Dietrich, W.E., Williams, R.M.E., Burr, D.M., Grant, J.A., Wilson, S.A., Matsubara, Y., 2014. Sedimentology and climatic environment of alluvial fans in the Martian Saheki crater and a comparison with terrestrial fans in the Atacama Desert. Icarus 229, 131–156.
Nanson, G.C., Croke, J.C., 1992. A genetic classification of floodplains. Geomorphology 4, 459–486.
Newsom, H.E., 2010. Heated lakes on Mars. In: Cabrol, N.A., Grin, E.A. (Eds.), Lakes on Mars. Elsevier, Amsterdam, pp. 91–110. http://dx.doi.org/10.1016/B978-0-444-52854-4.00004-0.
Newsom, H.E., Brittelle, G.E., Hibbitts, C.A., Crossey, L.J., Kudo, A.M., 1996. Impact crater lakes on Mars. J. Geophys. Res. 101, 14,951–14,955. http://dx.doi.org/10.1029/96JE01139.
Osterkamp, W.R., Hedman, E.R., 1982. Perennial-streamflow characteristics related to channel geometry and sediment in Missouri River basin. U. S. Geol. Surv. Prof. Pap. 1242 (37 pp.).
Parker, G., Paola, C., Whipple, K.X., Mohrig, D., 1998. Alluvial fans formed by channelized fluvial and sheet flow. I: theory. J. Hydraul. Eng. 124 (10), 985–995.
Pieri, D.C., 1980. Geomorphology of Martian valleys. In: Woronow, A. (Ed.), Advances in Planetary Geology. NASA/TM 81979, pp. 1–160.

Pondrelli, M., Rossi, A.P., Marinangeli, L., Hauber, E., Gwinner, K., Baliva, A., Di Lorenzo, S., 2008a. Evolution and depositional environments of the Eberswalde fan delta, Mars. Icarus 197, 429–451. http://dx.doi.org/10.1016/j.icarus.2008.05.018.

Pondrelli, M., Rossi, A.P., Marinangeli, L., Hauber, E., Baliva, A., 2008b. An application of sequence stratigraphy to Mars: the Eberswalde fan delta. In: Amorosi, A., Haq, B.U., Sabato, L. (Eds.), Advances in application of sequence stratigraphy in Italy. GeoActa, Special Publication 1, pp. 237–253.

Pondrelli, M., Rossi, A.P., Platz, T., Ivanov, A., Marinangeli, L., Baliva, A., 2011. Geological, geomorphological, facies and allostratigraphic maps of the Eberwalde fan delta. Planet. Space Sci. 59 (11–12), 1166–1178. http://dx.doi.org/10.1016/j.pss.2010.10.009.

Quantin, C., Allemand, P., Mangold, N., Dromart, G., Delacourt, C., 2005. Fluvial and lacustrine activity on layered deposits in Melas Chasma, Valles Marineris, Mars. J. Geophys. Res. 110, E12S19. http://dx.doi.org/10.1029/2005JE002440.

Ramirez, R.M., Kopparapu, R., Zugger, M.E., Robinson, T.D., Freedman, R., Kasting, J.F., 2014. Warming early Mars with CO_2 and H_2. Nat. Geosci. 7, 59–63.

Rice, M.S., Gupta, S., Bell III, J.F., Warner, N.H., 2011. Influence of fault-controlled topography on fluvio-deltaic sedimentary systems in Eberswalde crater, Mars. Geophys. Res. Lett. 38, L16203. http://dx.doi.org/10.1029/2011GL048149.

Rice, M.S., Bell III, J.F., Gupta, S., Warner, N.H., Goddard, K., Anderson, R.B., 2013. A detailed geologic characterization of Eberswalde crater, Mars. Mars 8, 15–59. http://dx.doi.org/10.1555/mars.2013.0002.

Sagan, C., Chyba, C., 1997. The early faint Sun paradox: organic shielding of ultraviolet-labile greenhouse gases. Science 276, 1217–1221. http://dx.doi.org/10.1126/science.276.5316.1217.

Schultz, P.H., Glicken, H., 1979. Impact crater and basin control of igneous processes on Mars. J. Geophys. Res. 84, 8033–8047.

Schultz, P.H., Schultz, R.A., Rogers, J., 1982. The structure and evolution of ancient impact basins on Mars. J. Geophys. Res. 87, 9803–9820.

Segura, T.L., Toon, O.B., Colaprete, A., Zahnle, K., 2002. Environmental effects of large impacts on Mars. Science 298, 1977–1980. http://dx.doi.org/10.1126/science.1073586.

Segura, T.L., Toon, O.B., Colaprete, A., 2008. Modeling the environmental effects of moderate-sized impacts on Mars. J. Geophys. Res. 113, E11007. http://dx.doi.org/10.1029/2008JE003147.

Segura, T.L., McKay, C.P., Toon, O.B., 2012. An impact-induced, stable, runaway climate on Mars. Icarus 220, 144–148. http://dx.doi.org/10.1016/j.icarus.2012.04.013.

Squyres, S.W., Kasting, J.F., 1994. Early Mars: how warm and how wet? Science 265, 744–749. http://dx.doi.org/10.1126/science.265.5173.744.

Toon, O.B., Segura, T., Zahnle, K., 2010. The formation of Martian river valleys by impacts. Annu. Rev. Earth Planet. Sci. 38, 303–322.

Wallace, D., Sagan, C., 1979. Evaporation of ice in planetary atmospheres: ice-covered rivers on Mars. Icarus 39, 385–400.

Warner, N., Gupta, S., Lin, S.-Y., Kim, J.-R., Muller, J.-P., Morley, J., 2010. Late Noachian to Hesperian climate change on Mars: evidence of episodic warming from transient crater lakes near Ares Vallis. J. Geophys. Res. 115, E06013. http://dx.doi.org/10.1029/2009JE003522.

Weitz, C.M., Bishop, J.L., Grant, J.A., 2013. Gypsum, opal, and fluvial channels within a trough of Noctis Labyrinthus, Mars: implications for aqueous activity during the Late Hesperian to Amazonian. Planet. Space Sci. 87, 130–145. http://dx.doi.org/10.1016/j.pss.2013.08.007.

Whiting, P.J., Stamm, J., 1995. The hydrology and form of spring-dominated channels. Geomorphology 12, 233–240.

Whitmire, D.P., Doyle, L.R., Reynolds, R.T., Matese, J.J., 1995. A slightly more massive young Sun as an explanation for warm temperatures on early Mars. J. Geophys. Res. 100 (E3), 5457–5464. http://dx.doi.org/10.1029/94JE03080.

Wilhelms, D.E., Baldwin, R.J., 1989. The role of igneous sills in shaping the Martian uplands. Proceedings of the Nineteenth Lunar and Planetary Science Conference. Lunar and Planetary Institute, Houston, TX, pp. 355–365.

Williams, G.P., 1988. Paleofluvial estimates from dimensions of former channels and meanders. In: Baker, V.R., Kochel, R.C., Patton, P.C. (Eds.), Flood Geomorphology. John Wiley and Sons, New York, pp. 321–334.

Williams, R.M.E., Malin, M.C., 2008. Sub-kilometer fans in Mojave crater, Mars. Icarus 198, 365–383. http://dx.doi.org/10.1016/j.icarus.2008.07.013.

Williams, R.M.E., Irwin III, R.P., Zimbelman, J.R., 2009. Evaluation of paleohydrologic models for terrestrial inverted channels: implications for application to Martian sinuous ridges. Geomorphology 107, 300–315. http://dx.doi.org/10.1016/j.geomorph.2008.12.015.

Wood, L.J., 2006. Quantitative geomorphology of the Mars Eberswalde delta. Geol. Soc. Am. Bull. 118 (5–6), 557–566. http://dx.doi.org/10.1130/B25822.1.

Wordsworth, R., Forget, F., Millour, E., Head, J.W., Madeleine, J.-B., Charnay, B., 2013. Global modelling of the early Martian climate under a denser CO_2 atmosphere: water cycle and ice evolution. Icarus 222, 1–19. http://dx.doi.org/10.1016/j.icarus.2012.09.036.